University of New Mexico
UNM Digital Repository

Electrical and Computer Engineering ETDs   Engineering ETDs

2-9-2010

Resource allocation of the human brain : a competitive equilibrium approach

Alexandre Rosa Franco

Follow this and additional works at: https://digitalrepository.unm.edu/ece_etds
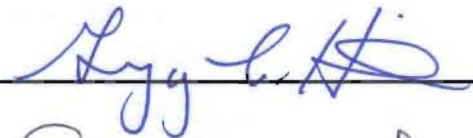
Alexandre Rosa Franco
_____
Candidate

Electrical and Computer Engineering
_____
Department
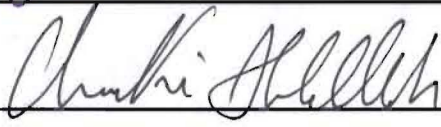
This dissertation is approved, and it is acceptable in quality and form for publication:

Approved by the Dissertation Committee:

_____ , Chairperson

_____

_____

_____

_____

_____

_____

_____

RESOURCE ALLOCATION OF THE HUMAN BRAIN:
A COMPETITIVE EQUILIBRIUM APPROACH

BY

ALEXANDRE ROSA FRANCO

Electrical Engineer, Pontifícia Universidade Católica do Rio
Grande do Sul, 2004

M.S., Electrical Engineering, Univeristy of New Mexico, 2005

DISSERTATION

Submitted in Partial Fulfillment of the
Requirements for the Degree of

Doctor of Philosophy
Engineering

The University of New Mexico
Albuquerque, New Mexico

October, 2009

Dedication

To my parents, Helenita and Paulo, for their unconditional love and support. They both have been great roll models not just to pursue of a doctorate degree but also to excel in all challenges of life.

"The important thing is this: To sacrifice what you are to what you could become. " – Charles DuBois

Acknowledgments

First, I would like to thank my advisor, Professor Gregory Heileman, for his support on this research and also for some great discussions about soccer and surfing. I would equally like to thank Dr. Andrew Mayer for this extensive teaching and support of the four years that I spent at the Mind Research Network.

I would also like to thank the remaining members of my doctorate committee, Dr. Vincent Calhoun and Dr. Chaouki Abdallah for their support and great ideas for this dissertation. Thank the Brazilian community in Albuquerque for their friendship and great churrascos. Thanks also for the great friendship from fellow students of the ISTEC lab.

Finally, I would like to thank my brother Eduardo and sister Carolina for being the best possible brothers that exist.

Resource Allocation Of The Human Brain: A Competitive Equilibrium Approach

by

Alexandre Rosa Franco

ABSTRACT OF DISSERTATION

Submitted in Partial Fulfillment of the
Requirements for the Degree of

Doctor of Philosophy

Engineering

The University of New Mexico

Albuquerque, New Mexico

October, 2009

Resource Allocation Of The Human Brain:
A Competitive Equilibrium Approach

by

Alexandre Rosa Franco

Electrical Engineer, Pontifícia Universidade Católica

do Rio Grande do Sul , 2004

M.S., Electrical Engineering, University of New Mexico, 2005

Ph.D., Engineering, University of New Mexico, 2009

Abstract

A novel model to study the resource allocation of a functioning brain is proposed. The mechanism is based on the theory of competitive equilibrium (CE), where users (cortical areas of the brain) are competing for a finite resource such as oxygenated blood. Concepts of CE are mathematically adjusted to be used with functional magnetic resonance imaging (FMRI) data. The current study uses imaging data were subjects are requested to selectively attend and respond to either a visual or auditory metronome in the presence of asynchronous cross-modal distractors. Two studies with distinct patient populations (patients with schizophrenia patients with mild traumatic brain injuries) are used to asses the applicability of the proposed method. Comparisons to traditionally used methods to analyze simulated and real FMRI data are also provided. Results indicate that it is possible to mathematically formulate an underlying resource allocation mechanism of a human

brain. Additionally, when comparing to traditional analysis methods, the proposed model increases the sensitivity of these data when examining different stimuli conditions and also increases the classification accuracy between the patient group versus normal controls.

Contents

Contents

Contents

Contents

List of Figures

List of Tables

Chapter 1

Introduction

A new method to analyze human brain functioning is introduced. This approach mathematically models the resource allocation inside the brain, making use of a game-theory concept, the theory of competitive equilibrium (CE). The proposed technique is based on a resource allocation mechanism widely used and developed in financial interactions [20]. More recently, the same resource allocation model has been applied to explain resource allocation in communication networks [25, 40]. With the use of functional magnetic resonance imaging (FMRI), we are capable of observing the distribution of physical resources, such as glucose and oxygen in the brain. A model that directly assesses the resource allocation of the brain seems realistic and appropriate. With the proposed method, the interactions of brain cortical areas under different scenarios is observed. In this model, cortical areas are thought of as of "competing" for resources. Additionally, a measurement of relative activation is defined and used to compare brain functionality across different stimuli conditions. The model is tested on two FMRI experiments, a rate (RATE) experiment and a mulitimodal attention task (MMAT) experiment. The RATE study was conducted with healthy normal controls (NC) as well as with patients who suffer from schizophrenia (SZ). The MMAT study is also with normal controls, but also includes patients who have suffered a mild traumatic brain injury (mTBI). This is a multisession study, where subject are

scanned twice, three to five months apart between each FMRI session.

1.1 Motivation

Similarities in the organization of the brain and electronic or communication networks has been discussed in detail by Laughlin and Sejnowski [27]. They state: "... (brain) structure and function are governed by basic principles of resource allocation and constraint minimization, and that some of these principles are shared with human-made electronic devices and communication networks." They also suggest that energy supply limits signal traffic in the brain. This is a strong indication that the brain must have an underlying resource allocation mechanism. Other studies suggest that the brain is organized similar to a communication network, where the human cortex is compared to small world networks [39, 4]. Others have argumented that the brain can also be modeled as a complex network [2]. However, these studies focus mainly on brain structure, comparing them to human made networks. On the other hand we wish to study the efficiency of the brain in a functional sense, and observe how resources are allocated throughout the brain during different experiment conditions. To our knowledge, the brain has not been studied from this perspective.

Humans can only attend to a limited amount of simultaneous stimuli [34], therefore some underlying allocation mechanism based on priorities is likely to be implemented in the brain. For example, if a person is listening to music with their eyes closed, the primary auditory cortex shall receive more resources than the visual cortex. Additionally, a human's ability to multitask is severely limited [14], especially when the tasks require a higher-level of attention. Other indications that the brain has an internal resource allocation mechanism is that the brain is limited in its information processing capabilities [29], where it is considered that the brain is limited because of a bottleneck in the passage of information in some cortical areas. Furthermore, indications that a functional resource

allocation is occurring in the brain can be seen in Kelly et al. [24]. They showed that there is a direct negative temporal relationship in the BOLD response between task positive and task negative networks, indicating that brain networks cannot all be active at the same time, even at rest.

The resource allocation mechanism that is proposed is based on a theoretical competitive equilibrium (CE) approach, a means to mathematically equate how resources are allocated. With CE, allocation of resources is based on the total amount available resources of the system and also a "utility function" for each of the brain regions. Cortical areas are considered to be competing for resources based on the "value" they give to the resource. Unlike traditional methods that examine the absolute activation of cortical areas, with this proposed method, the brain is viewed as a distributed mechanism. We are ultimately trying to uncover the mechanism inside the brain that governs the allocation of resources, a reverse engineering problem. A detailed description of CE is introduced in chapter 3.

1.1.1 Brain Equilibrium

To study the brain as an efficient resource allocation mechanism, we must understand how it reaches a resource allocation equilibrium. By equilibrium, we can state that the brain has reached a stable point, where through several changes (growth in size, reorganization or plasticity) it reaches a point where no major structural and functional changes will occur. This project mainly focused on the equilibrium of the attentional system. One perspective that can be hypothesized is stabilization through normal growth of the brain from childhood to an adult age (i.e., *pruning*).

The structure of the brain is relatively the same in all normal adult humans, with some small variations on the gyri folding and brain size. Structure is predetermined by our genetic sequence. What makes us have unique personalities is the fact that the internal "wiring" is different for each individual. This is due to the synaptic formation that occurs

between neurons. The number of synapse in the human cortex is in the order of 10^{14} [26]. It is believed that it is impossible that our genetic program could assign all these connections, where only a general outline of the circuitry is encoded.

There is a large increase in synaptic density between embryonic life up to the age of two in humans. Typically around the age of two is when humans have the highest concentration of synapses followed by a plateau in density. Subsequently there is a large decrease in synapses, characterized as pruning. This large organization of the circuitry occurs up to the end of puberty. However, the rate of creating and pruning of synapses is not homogenous, where in the sensorimotor regions the process occurs earlier and in higher cognitive areas the process is delayed. Reduction in synapses is dramatic; the number of synapses at the end of puberty may fall to 50% compared to at the age of two. There is a loss of up to 100,000 synapses per second in adolescence [26]. During adulthood, existing circuits are still being modified (i.e., creating new memory) but at a much slower pace. A detailed analysis of synaptic pruning can be seen in [26]. A cartoon scheme of synaptic density in the human cortex is shown in Figure 1.1.

There are two general mechanisms of synaptic pruning, *experience expectant* and *experience dependent* [26]. Experience expectant depends on the presence of certain sensory experiences for the organization of the synapses. Usually, these patterns are the same for members of the same species. For example, in the visual cortex synaptic formation is dependent on exposure to features such as line orientation, color and movement. Experience dependent pruning occurs based on unique personal experiences, such as speaking a distinguished language. Circuitry of the frontal lobe is believed to be formed by experience dependent pruning. Therefore it is believe that the sensorimotor cortex in an adult human should have a similar structure since most are exposed to some common stimuli (i.e., seeing, hearing and touching). Higher cognitive mechanisms may be more subject dependent.

A study by Casey [9] showed that the prefrontal cortical activity in children was up to
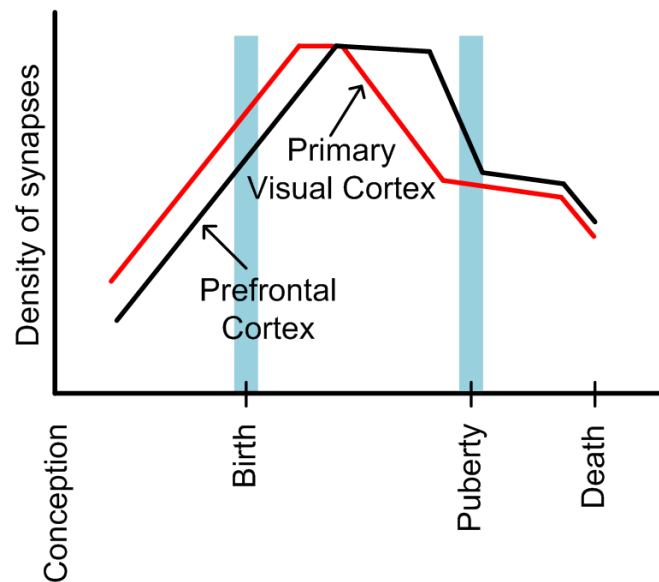
Figure 1.1: Changes in density of synaptic connections in the prefrontal correct and in the primary visual cortex of a healthy human.

four times larger compared to adults. Two theories were conceived by these results; with age, cortical areas may become more specific with experience, while another interpretation is that the task was more difficult to children, therefore required more activation. The first theory would speculate that a child's brain is disorganized and function assignments of cortical areas are not well defined. Another report by Casey [8] showed that "immature cognition is characterized by an enhanced sensitivity to interference from competing sources (e.g., response competition)." In addition, experience-driven maturation process "reflects fine-tuning of the neural systems with experience and development [8]." Finally, pruning and elimination of connections with strengthening of relevant ones contribute to cognitive maturation.

Based on these findings it is possible to interpret that the brain starts as a system without any organization (large density of synapses) and with life experience a equilibrium is reached. Since the equilibrium or organization is also based on life experience, every

person is at a different equilibrium point, especially at higher cognitive areas of the brain. However, we can hypothesize that the sensorimotor system in a normal adult should have a similar configuration, since the pruning in these areas is experience expectant.

1.1.2 Development of the Patient Brain

A deviation from a normal development to equilibrium (i.e., resource allocation) might be expected from patients that suffer from schizophrenia. An "optimal" distribution of resources for the patient group might differ from the "optimal" of adults who do not suffer from any mental disease. In addition, a patient who suffers a traumatic brain injury might be subject to an unbalance in the normal "equilibrium" state. During maturity the pruning process is considered to be normal. However, subsequent to suffering a head injury, this equilibrium might be shifted. On the other hand, patients that suffer a minor injury are capable of recovering to an optimal distribution of resources of the attentional system. Therefore, the balance of how resources are allocation in the patient groups might defer from NC. A hypothetical flowchart is seen in Figure 1.2.

An array of symptoms characterize a person suffering from schizophrenia; such as hearing internal voices or experiencing other sensations not connected to an obvious source (hallucinations), disorganized speech, and assigning unusual significance or meaning to normal events or holding fixed false personal beliefs (delusions) [26]. It is believed that schizophrenia is a developmental disease, where an "analysis of home movies showed that people who later developed schizophrenia have shown subtle, but reliable, disturbance in a variety of behavioral types (motor, cognition, social) many years before there are clinical symptoms of schizophrenia [28]". As an example, the auditory mechanism might be altered compared to NC. This motivates the use of a resource allocation mechanism to attempt to understand the interaction between neuronal areas of SZ.

For patients who suffer a minor traumatic brain injury (mTBI), we hypothesis that
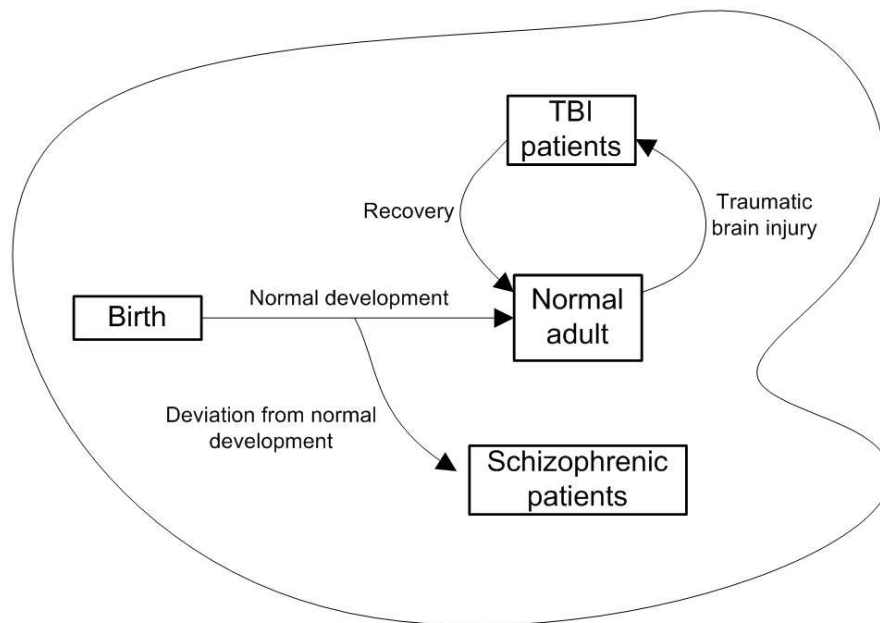
Figure 1.2: Theoretical flowchart of development to a equilibrium of the attentional system in the human brain and how other equilibriums are reached in patient groups.

the equilibrium of the brain is perturbed because of the accident, and through plasticity, recovers over time to the optimal resource allocation mechanism. Therefore we would expect to see significant differences in the resource allocation between mTBI patients and NC immediately following injury and no differences 6 months to 1 year later. Post injury symptoms injuries include but are not limited to problems with executive functioning, working memory and attention [5, 32]. On Kaas's paper on plasticity of motor and sensory maps [23], results show that in mammals the sensory maps are reorganized following lesions. Kaas also states that sensory maps in the somatosensory, visual, and auditory systems are capable of change in location. This reorganization can occur within hours up to many months. Even though plasticity is much more pronounced in children, it still occurs in adults post-head injury. Plasticity can also be considered as a restructuring of the synaptic connections in the brain. Therefore, the use of patients with traumatic brain injuries is advantageous to test the proposed resource allocation mechanism, since there

is a change in equilibrium following injury. However, typical symptoms of patients with mTBI usually disappear 3-5 months post injury. Consequently, the proposed method could be used again to test if a "normal" equilibrium is achieved.

It is important to note that it is beyond the scope of this dissertation to define the reasons why people suffer from schizophrenia and acquire symptoms post mTBI, however, this project is attempting to create new method that might help understand the disease and recovery respectively.

1.2 Proposed Model

To evaluate and test the proposed model we used two FMRI experiments. The first experiment (RATE) was performed on NC and SZ, where two conflicting stimuli are presented in a block design, an auditory tone and a flashing checkerboard [30]. Stimuli are presented in three different frequencies (0.5, 1.0, 2.0 Hz). Allocation of resources is observed based on whether the subject is told to attend to one modality (auditory or visual stimuli) when a conflicting stimulus is present. We predict that as there is an increase in the rate of the stimulus, there is an increase of the specificity of how resources are allocated. The second experiment (MMAT) consists of a similar experiment with two conflicting stimuli. However, now the patient group has suffered a mTBI. Additionally, participants were now asked to correctly identify a target number (one, two or three) presented in one sensory modality (auditory or visual) while ignoring the stimuli presented in the opposing sensory modality by pressing a button. Further details of the experiments are giving in chapter 2.

A comparison to traditional FMRI analytical methods is also provided to emphasis the advantage of using this new model to analyze FMRI data. This is done to test the sensitivity and specificity of the proposed model. The most widely used methods for studying brain behavior only analyze direct condition-by-condition behavior. Scalar values of the hemo-

dynamic response are usually obtained through multiple regression [17] or a deconvolution analysis [18]. Typically, statistical tests are performed then directly on the multiple regression beta coefficients (β) or percent signal change (PSC) of each voxel depending on the condition. Additionally, since the task involves different rates of the stimuli, we also are capable of looking at the slope of the activation, where the hemodynamic response is assumed to be monotonic in relation to the stimulus [38].

1.3 Aims

In summary, the current study has three aims:

- *Aim 1: Resource Allocation of the Brain*

  The first aim is to develop a resource allocation model of brain function as measured by FMRI. This model incorporates the "importance" of receiving resources of each neuronal area based on whether the subject is instructed to attend to one of the sensory modalities.

- *Aim 2: Resource Allocation in Patient Groups*

  The second aim of this project is to observe if there is a deviation of resource allocation in two patient populations. Results from other traditional methods such as statistical tests on the hemodynamic respose will be evaluated and compared to the resource allocation model.

- *Aim 3: Classification*

  A third and final aim will be to perform classification with features extracted from the resource allocation mechanism. With the use of a machine learning technique (e.g., support vector machine), classification between groups will be evaluated to test the performance of the resource allocation mechanism as a feature extraction tool.

1.4   Outline

Chapter 2 presents the FMRI experiments that are used to evaluate the resource allocation model. The experiments and subject population are explained in detail. Also, the FMRI data processing pipeline is presented. Chapter 3 introduces the proposed resource allocation method. With the use of the FMRI experiments, mathematical models of resource allocation are presented. Chapter 4 presents results of using the resource allocation model on the two experiments. Results of statistical tests across conditions and also across patient populations are shown. Classification results using the resource allocation model as a feature extraction tool are also presented. Additionally, results from other traditional methods used in FMRI studies are also shown. In chapter 5 a discussion of the results is presented and future direction in the study of resource allocation of the human brain are discussed.

Chapter 2

FMRI Data and Preprocessing

2.1 Rate Study

The goal of the RATE study was to understand the selective attention brain mechanism In patients with schizophrenia (SZ) a also heathy normal controls (NC)is also evaluated. A paper discussing the results of a neurological assessment of this experiment on NC has been previously published [30]. A detailed discription of the study is shown as follows.

2.1.1 Subjects

This study evolved studying patients with SZ and NC while undergoing a FMRI session. All SZ subjects were diagnosed by an experienced clinician or team member with the Structured Clinical Interview for DSM-IV Axis-I Disorders, Clinician Version (SCID-CV). Sixteen SZ (15 male, 1 female) and 16 NC (15 male, 1 female) participated in the experiment. One female NC subject was identified as an outlier (excessive motion; above 3 standard deviations [31]) and was excluded from further analysis along with the matched SZ. SZ with a history of other neurological disease, a history of psychiatric hospitalizations

within the previous six months or a history of substance abuse within the past year were excluded from the study. SZ were also required to be stable on an atypical, anti-psychotic medication (Aripiprazole 4; Ziprasidone: 1; Risperidone: 5; Quetiapine Fumarate: 4; Olanzapine: 2) for at least three months to be included in the current study. All HC were screened and excluded from the study based on a history of major medical conditions, neurological disease, major psychiatric disturbance, substance abuse or psychoactive pre-scriptive medications usage. There were no significant differences ($p > 0.10$) between SZ and the remaining HC for all major demographic categories including age (SP: 40.2 $\pm$ 8.2, HC: 40.1 +/- 8.8), education (SP: 12.6 +/- 2.4, HC: 13.0 +/- 1.4), or handedness (SP: 77.7 +/- 56.1, NC: 67.3 $\pm$ 68.9) as assessed by the Edinburgh Handedness Inventory [35]. Informed consent was obtained from subjects according to institutional guidelines at the University of New Mexico and the New Mexico Department of Veterans Affairs. This study is concluded and no more data will be collected.

2.1.2   Tasks

All stimuli were presented in a blocked design format. Prior to each block, there was a baseline period in which a white fixation cross in the center of the projection was presented on a black background. Subjects were requested to maintain fixation on the cross during the experiment. To prevent the development of temporal expectations and to allow for the best sampling of the hemodynamic response in the regression model [6], the duration of the baseline period was randomly varied between 10 and 14 s . During the task, participants were instructed to bimanually tap their fingers into an input device in synchrony with the onset of a reversing checkerboard (duration = 100 ms) and/or a pure tone (1000 Hz with a 10-ms linear rise and fall; duration = 100 ms) that were presented at intervals of 2000 (0.5 Hz), 1000 (1 Hz), or 500 ms (2 Hz).

In the *attend-both* condition, auditory and visual stimuli were simultaneously pre-

sented at the same frequency (0.5, 1.0, or 2.0 Hz), and subjects were instructed to attend to and tap in synchrony with the auditory and visual stimulus. In the *attend-auditory* and *attend-visual* conditions, subjects were instructed to selectively attend to, and tap in synchrony with, either an auditory or a visual stimulus, respectively, while ignoring the stimulus in the other modality. In both the attend-auditory and attend-visual conditions, the stimulus in the ignored modality always occurred at a different frequency. The ignored stimulus always occurred either in or out of phase with the attended stimulus across the 8 second trial duration. Specifically, there were two trial types for each attended stimulus rate based on the frequency of the unattended modality (e.g., attended auditory stimuli at 0.5 Hz were always paired with visual distracters occurring at either 1.0 or 2.0 Hz). Trial order was pseudorandomized across all six functional neuroimaging runs. A description of a stimulus block is shown in Figure 2.1.

Figure 2.1: A diagrammatic representation of the trial structure for a representative of the attend both stimulus block for the RATE study.

2.1.3   MR Imaging

At the beginning of the scanning session, high resolution T1 (time echo [TE] = 4.76 ms, repetition time [TR] = 12 ms, $20°$ flip angle, number of excitations [NEX] = 1, slice thickness = 1.5 mm, field of view [FOV] = 256 mm, resolution = 256×256) anatomic images were collected on a 1.5-Tesla Siemens Sonata scanner. For each of the 6 imaging series, 201 echo-planar images were collected using a single-shot, gradient-echo-planar pulse sequence (TR = 2000 ms, TE = 36 ms, flip angle = $90°$, FOV = 256 mm, matrix size = 64 3 64). The first image of each run was eliminated to account for T1 equilibrium effects, leaving a total of 1200 images for the final analysis. Twenty-eight contiguous sagittal 5 mm thick slices were selected to provide whole-brain coverage (voxel size: $4 \times 4 \times 5$ mm).

2.2   Multimodal attention task (MMAT) study

The objective of this study was to analyze the effect on the brain of people who suffer a mild traumatic brain injury (mTBI) and analyze their recovery. This is an ongoing study and subject data are still being collected. Additionally, this is a multisession study, where subjects are asked to return for a second FMRI session after 3-5 months from the first session so that the recovery from the brain injury can be evaluated.

2.2.1   Subjects

Semi-acute mTBI (within 3 weeks) patients were recruited from our regional trauma one center at the University of New Mexico Hospital. All mTBI subjects were scanned within 21 days of their accident and experienced a mental status change following the trauma. Specific inclusion criteria for the study were based on the American Congress of Rehabilitation Medicine and included a Glasgow Coma Score of 13-15 at the initial assessment

in the emergency room, loss of consciousness (LOC) if present was limited to 30 minutes, and post-traumatic amnesia was limited to a time gradient of 24 hours. Subjects and matched controls were excluded from the study if there was a positive history of a neurologic or psychiatric disease, substance/alcohol abuse, learning disorder, attention deficit hyperactivity disorder, or a history of a head injury with a LOC of greater than 5 minutes. Informed consent was obtained from all participants following guidelines set by the University of New Mexico. Up to the date of the conclusion of data analysis (August 14th, 2009) at least 24 patients and 27 healthy controls have been scanned. Additionally, 10 patients and 27 healthy controls have participated in a second FMRI session. Therefore, 24 mTBI subjects and their matched NC (age, years of education, gender) are evaluated for the first visit, and only 10 mTBI subjects and their matched NC are examined for the second visit.

2.2.2   Tasks

Participants underwent a FMRI task in which they were simultaneously presented with auditory and visual stimuli (numbers) occurring at two different frequencies (.33 or .66 Hz) over a 9 second block (Figure 2.2). Participants were asked to correctly identify a target number (one, two or three) presented in one sensory modality (auditory or visual) while ignoring the stimuli presented in the opposing sensory modality by pressing a button as quickly and accurately as possible. The multimodal stimuli were either identical (congruent condition) or conflicting (incongruent condition). Only the incongruent condition is analyzed in this dissertation. Prior to the presentation of the target numbers, a cue word was presented to indicate the modality for focused attention. The cue for the auditory modality was "HEAR" and the cue for the visual modality was "LOOK." There were also passive attention trials in which the participant did not need to attend either modality, and the cue for those trials was "NONE." For example, if the cue was "HEAR," participants responded to the target numbers in the auditory modality while ignoring visual stimuli.
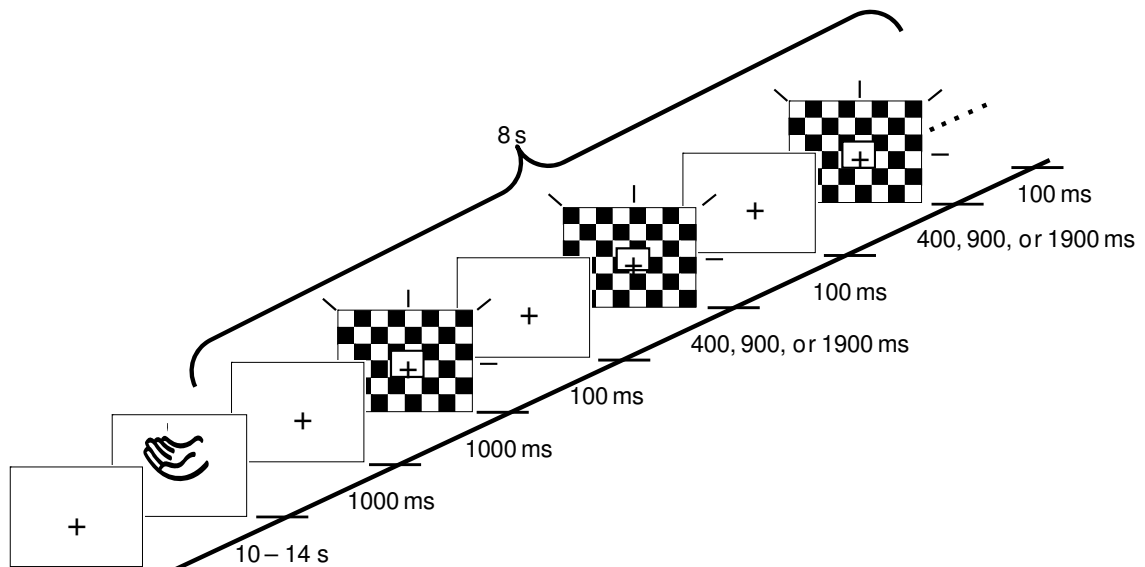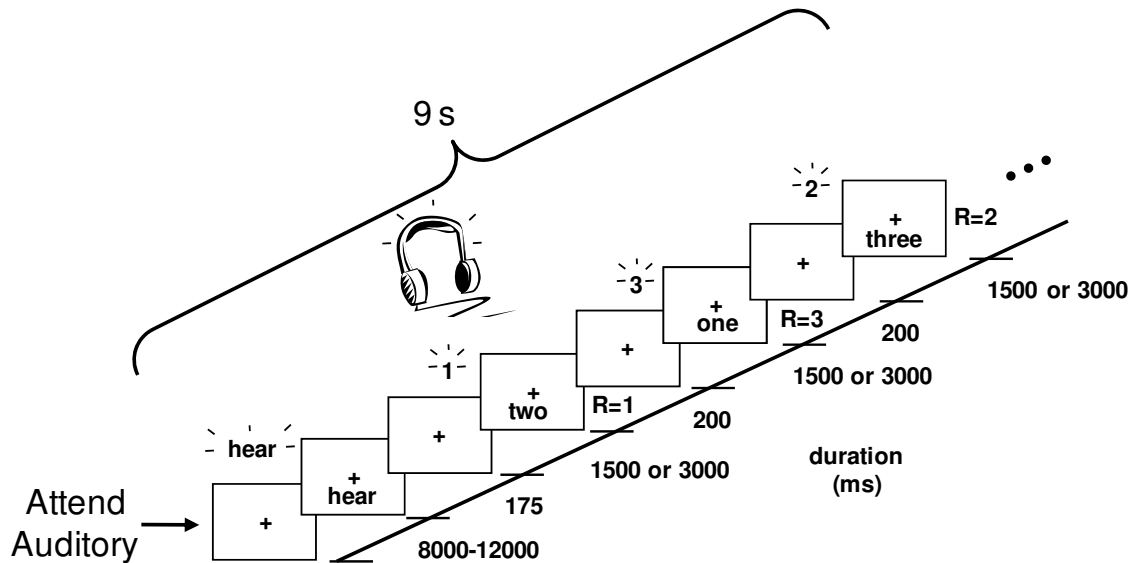
Figure 2.2: A diagrammatic representation of the trial structure for a representative incongruent stimulus block for the MMAT study.

All visual stimuli were presented in word rather than Arabic form, since words produce more interference in numeric Stroop tasks [16]. To permit the full allocation of attentional resources, the stimulus onset asynchrony (SOA) between the presentation of the cue and the stream of target numbers was 1000 ms. To establish a baseline resting state in the regression model the time between trials was randomized between 8, 10 and 12 seconds [6]. Presentation software was used to control stimulus presentation, synchronization of stimulus events with the scanner, and the collection of accuracy of the responses and reaction time (RT) data for offline analysis.

2.2.3   MR Imaging

High resolution T1 (TE (echo time) = 1.64 ms, TR (repetition time) = 2.53 s, $7°$ flip angle, number of excitations (NEX) = 1, slice thickness = 1 mm, FOV (field of view) = 256 mm, resolution = 256 x 256) anatomic images were collected on a 3 Tesla Siemens Trio

scanner at the beginning of each experiment. For the six FMRI series, 162 echo-planar images were collected using a single-shot, gradient-echo echoplanar pulse sequence (TR = 2000 ms; TE = 29 ms; flip angle = $75°$; FOV = 240 mm; matrix size = 64 x 64). The first image of each run was eliminated to account for T1 equilibrium effects, leaving a total of 1127 images for the final analyses. Thirty-three contiguous sagittal 3.5 mm thick slices with a gap factor of 1.05 mm were selected to provide whole-brain coverage (voxel size: 3.75 x 3.75 x 4.55 mm).

2.3   Functional Image Processing

Most of the FMRI data were analyzed in a hierarchical fashion using AFNI [11], a widely used freeware software for FMRI analysis. Additional processing (registration) was performed using FSL [21]. Preprocessing of both datasets are identical unless stated. In Figure 2.3 an outline of the preprocessing is shown.
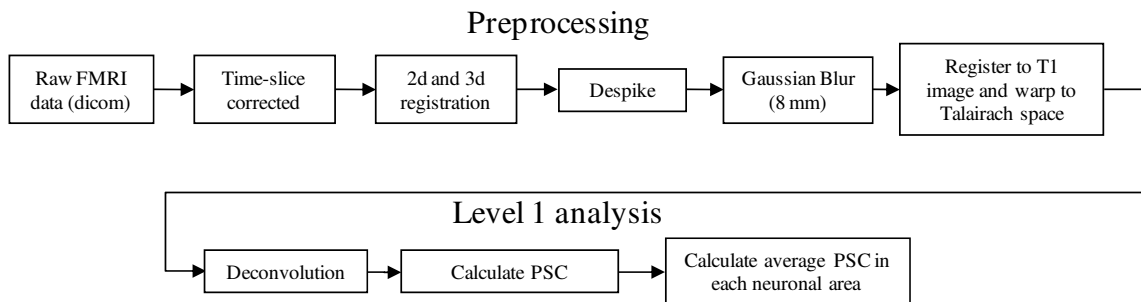
Figure 2.3: FMRI preprocessing pipeline.

During the collection of FMRI data, each slice is acquired at a different time point within the scanner. Therefore, the six individual task time-series were first temporally aligned using a sinc interpolation to ensure that all data had the same temporal origin. Second, the four-dimensional images were subsequently spatially registered to the second image from the first task run (i.e., first image that was not contaminated by T1 equilibrium

effects) in both two- and three-dimensional space to minimize effects of head motion. Retrospective motion correction techniques can be conceptualized as occurring in two distinct steps, motion detection and the subsequent correction of this motion [11, 3, 12]. Assumptions are based on the of stability in contrast values between successive images. Relatively small movements compared to image resolution can be fixed using this method. Motion is modeled according to six rigid-body parameters. In the detection phase, a cost function,

$$C = \sum_{V} \left(I(v) - R(v) \right)^2 \tag{2.1}$$

which is posited to be an index of spatial displacement, is calculated between the image of interest (I) and the reference image (R) across all voxels v. An iterative optimization algorithm (typically a least-squares fit) is then implemented to minimize the cost function, thereby reducing the spatial displacement between the two images. During the correction phase, the image of interest is interpolated to a new spatial grid specified by the optimization solution using a sinc function, correcting for the differences in spatial displacement.

Third, random spikes in the voxel time series due to machine or other artifacts were eliminated. This was accomplished by first fitting the time-series of each voxel to a smoothed curve. Next, the median absolute deviation (MAD) of the differences between the data time series and the smoothed curve is calculated. For each time point of the voxel

$$s(t) = (x(t) - c(t))/\sigma \tag{2.2}$$

is calculated, where $x(t)$ is the original BOLD intensity at time t, $c(t)$ is the smoothed fitted curve at time t and σ is the standard deviation of the residuals that is computed by

$$\sigma = \sqrt{\pi/2} \cdot MAD. \tag{2.3}$$

Any $s(t)$ that is greater than 2.5 is replaced by

$$s'(t) = 2.5 + 1.5 \tanh((s(t) - 2.5)/1.5). \tag{2.4}$$

Fourth, the data was spatially blurred using a 8 mm Gaussian full-width half-maximum filter to improve the signal-to-noise ratio [36] and to increase compliance with random field models [17]. All the images were then spatially registered to the anatomical T1 image using a 12-parameter affine transformation and converted to a $1mm^3$ standard stereotaxic coordinate space [41].

A deconvolution analysis [18] was used to generate one impulse response function (IRF) for each of the 15 selective attention condition on a voxel-wise basis. For the RATE study, each IRF was derived from the first twelve images (22 seconds) following the onset of the cue (total trial length varied from 20 to 24 seconds). The peak images (eight to twelve seconds post-stimulus onset) of the resultant IRFs were then compared against the baseline period (i.e., maintaining visual fixation) to create the percent signal change (PSC). In the MMAT study, the IRF was derived from the first 8 images and the peak was selected from the fourth to the eight second post-stimulus. The PSC values were used to evaluate the resource allocation of the brain as is shown in the next chapter.

For the RATE dataset, data were then averaged to simulate that the subject was attending to a stimulus and ignoring the other at the same frequency. With signal averaging, a direct comparison of activation when the subjects are instructed to attend to the auditory or visual while ignoring a cross-modal stimuli at the same frequency is permitted. The hemodynamic response is assumed to be monotonically increasing with the increase of the

stimuli at the frequency range that is being used (0.5 to 2.0Hz) [38]. As an example, in the attend auditory condition, the subject is instructed to attend to a auditory tone at 0.5 Hz, while the visual stimulus is either at 1.0 or 2.0 Hz. Another condition is that the subject is instructed to attend to an auditory stimulus at 1.0 Hz and ignore a visual stimulus at 0.5 or 2.0 Hz. Therefore if we calculate the average PSC's of the attend auditory at 0.5 Hz/ignore visual 1.0 Hz and attend auditory at 1.0 Hz/ignore visual 0.5 Hz we will simulate that the subject is attending to a auditory stimulus at 0.75 Hz and ignoring the visual stimulus at the same frequency. With these signal averages, the new rate of attended and ignored frequencies are at 0.75, 1.25 and 1.5 Hz. The same calculations are performed for the attend both condition to maintain consistency in the stimuli frequency. Additionally, the slope of activation is also calculated across these three new frequencies. For the MMAT study, no signal averaging is necessary since the frequency of the attended and ignore signals are the same.

Chapter 3

Resource Allocation of the Brain

Resource allocation of an infinitely divisible resource in an FMRI framework is presented in this section. The model is presented to fit the Rate study framework, however the concepts and equations are easily adjustable to the MMAT study. Competitive equilibrium (CE) [25] finds a distribution of a resource that maximizes the aggregate utility among the users r, were $r = 1, 2, ..., R$. We define the "users" as the cortical areas of the brain that are competing for a resource. R is the total number of cortical areas that the brain is segmented into. The brain was segmented into fifty regions to define the users based on the Talairach atlas [41] (see Figure 3.1). Segmentation was obtained from AFNIs TTatlas (http://afni.nimh.nih.gov/afni/doc/misc/afni_ttatlas/). The brain is divided into 50 areas and based on previously defined cortical areas, were each cortical area is individually color-coded. Segmentation does not defer between hemispheres, therefore areas of both sides are considered as one user. The list of neuronal regions are shown in Table 4.3. It is important to note that the brain is only segmented in gray matter areas and not white matter. Gray matter is where the true processing of information occurs in the brain while the white matter is only responsible for transmission of information between gray matter cells [26]. Other possible segmentation of brain into 66 regions is proposed by Desikan [13], were it was further segmented into 998 regions by Hagmann [19]. Another possibility

is to segment areas based on the functional data. This can be preformed using group ICA [7], were each resulting independent component can be used as a mask to define the users of the resource allocation model.
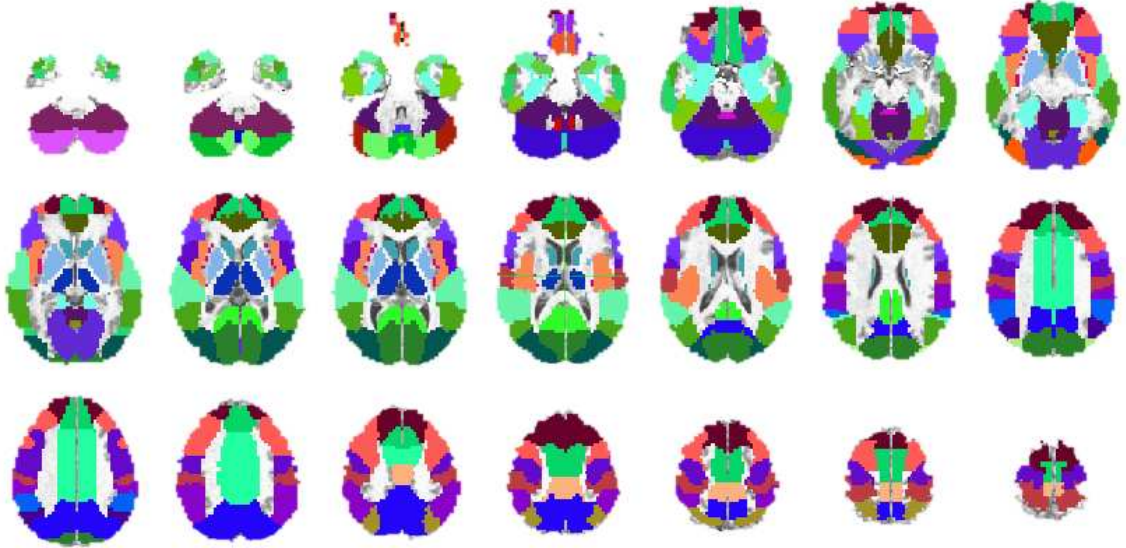
Figure 3.1: Segmentation of brain regions to create users.

The distributed resource is measured as the level of the hemodynamic response (PSC), here defined as $d_{r,f}$. A utility function $U_r(d_{r,f})$ can be seen as the "value" or "importance" that the cortical area r furnishes while receiving a portion of the resource, $d_{r,f}$, at each stimulus frequency f. An area will have a different utility function based on three conditions; however, the function will be the same throughout the frequencies. As an example, the "importance" function of receiving resources in the visual cortex does not change based on the rate of the stimulus, but it does change based on whether or not the subject is instructed to attend to the visual stimulus or not. The whole supply of resources that will be divided among the neuronal areas is represented by S_f.

To simplify the presentation of the model and also without loss of generality, we will address only one stimuli condition, where the subject is instructed to attend the auditory stimulus and ignore the visual stimulus. A mechanism is created to define how the resource

are subdivided among the cortical areas. To distribute the resources among the regions, the following optimization problem can be addressed, where a social welfare function is maximized at each distinct frequency

$$Maximize_f \quad \sum_r U_r(d_{r,f}) \tag{3.1}$$

The social welfare function is viewed here as the sum of all the utilities of the regions based on the proportion of resources they receive. However, there are some constraints that must be complied with

$$\sum_r d_{r,f} \leq S_f \tag{3.2}$$

$$d_{r,f} \geq 0 \tag{3.3}$$

where the sum of the resources given to the cortical areas cannot be greater than the total available supply (Eq. 3.2). In addition, cortical areas are not capable of supplying resources to the system (Eq. 3.3). As modeled here, the system (brain) always attempts to optimize the distribution of resources to the neuronal areas based on the areas' utilities and the total available supply to all of the brain. S_f is variable, since there is a change in the total supply (oxygenated blood and glucose) to the whole brain dependent on the frequency of the stimuli and on one of the three condition. The optimal allocation of resources can be found using Lagrangian multipliers. Distribution of the allocation of the resource is defined by the vector $\mathbf{d} = (d_1, ..., d_R)$, and the optimal distribution is defined by $\mathbf{d}^* = (d_1^*, ..., d_R^*)$. As stated before, it is assumed that the brain always tries to optimally distribute resources (find $\mathbf{d}^*$) depending on the environment the person is encountering.

The utility function $U_r(d_{r,f})$ for each area r, over the domain $d_{r,f} \geq 0$, is assumed to be continuously differentiable, non-decreasing and is a strictly concave function. Since

the objective function is continuous and the feasible region is compact, a unique optimal solution $\mathbf{d}_f^*$ exists, where:

$$\sum_r U_r(d_{r,f}^*) \geq \sum_r U_r(d_{r,f}) \ \forall \, \mathbf{d}_f \tag{3.4}$$

is satisfied for any other resource allocation distribution, and $\mathbf{d}^*$ is unique.

3.1 Defining the Utility Function

A general class of utility functions that satisfies the previous defined requirements to obtain a unique solution (Eq. 3.4), is defined as [40]:

$$U_r(d_r) = w_r \frac{d_r^{1-\alpha}}{1-\alpha} \tag{3.5}$$

The variable w_r is viewed as the weighting factor of the utility function. This is the key point of the utility function which defines the "importance" that each neuronal region gives to the resource being distributed. Therefore each area will have a different w_r. Parameter α changes the shape of the utility function. α is addressed in more detail later in this chapter.

3.1.1 Calculating the Weights

As noted before, the utility function of each area does not change based on the rate of the stimulus, but rather according to different conditions. From Eqs. 3.1, 3.2, and 3.3, and incorporating the general class of utility functions (Eq. 3.5) we obtain for each frequency:

$$Maximize_f \quad \sum_r w_r \frac{d_{r,f}^{1-\alpha}}{1-\alpha} \tag{3.6}$$

$$\sum_r d_{r,f} = S_f \tag{3.7}$$

$$d_{r,f} \geq 0 \tag{3.8}$$

Another change from the original equations is that now it is assumed that all the resources are exhausted, as seen in Eq. 3.7. To find the optimal distribution, Lagrangian multipliers are calculated for each frequency [15]:

$$L(\mathbf{d}_f, \lambda_f) = \sum_R w_r \frac{d_{r,f}^{1-\alpha}}{1-\alpha} - \lambda \left(\sum_R d_{r,f} - S_f \right) \tag{3.9}$$

To find the maximum of Eq. 3.6 constrained to 3.7 and 3.8, the derivative of Eq. 3.9 in relation to d_r is calculated and set equal to zero:

$$\frac{\partial L(\mathbf{d}_f, \lambda_f)}{\partial d_{r,f}} = w_r d_{r,f}^{-\alpha} - \lambda_f = 0 \tag{3.10}$$

Therefore:

$$d_{r,f} = \sqrt[\alpha]{w_r/\lambda_f} \tag{3.11}$$

In economic terms, the λ_f is viewed as the price per unit of the resource, where in functional imaging, λ_f is an proportional inverse of availability of resources. Additionally, from Eq. 3.11, as λ_f increases, the resources received by each area $d_{r,f}$ decreases.

However, there is no way to directly calculate λ_f using functional imaging, as it is something internal to the system (brain). A solution to this problem is to first create a new user, which is defined as the whole brain (WB). First, we fix $w_{WB} = 1$, and with the WB PSC we solve for λ_f ($\lambda_f = S_f^{-\alpha}$) in Eq. 3.11. Other means to define the value of S will be addressed in future projects. The use of a different constant value (w_{WB}) does not effect any changes in the final results, since it is only a relative value. Additionally, we are favored by using this method. By fixing a value of the WB weighting factor, then calculating λ_f, a reference weighting factor is created. Therefore, cortical areas that have a higher PSC compared to the average of the brain will receive a $w_r > 1$. Also, since a different λ_f is calculated for each subject, the cortical weighting factors of each subject are relative to the subjects' WB activation.

With λ_f's defined, the weighting factor can be calculated for each region. Since the weighting factor w_r is assumed to be a constant across all frequencies, the weight is calculated from an average from all frequencies:

$$w_r = \frac{1}{3} \left(\lambda_{0.75Hz} d_{r,0.75Hz}^{\alpha} + \lambda_{1.25Hz} d_{r,1.25Hz}^{\alpha} + \lambda_{1.5Hz} d_{r,1.5Hz}^{\alpha} \right) \tag{3.12}$$

Therefore, the w_r for each cortical area can be calculated. Statistical tests with the weighting factors can be performed to compare resource allocation associated with each of the three conditions. In addition, these results can be compared to traditional methods, such as directly comparing the PSC and the slope across different experimental conditions. Also, the weighting factors are the features to be used in the classification of groups.

However, an α value must still be defined for the utility function (Eq. 3.5). Since we are performing a reverse engineering problem, the α parameter must be found that best mimics how the distribution of resources are actually occurring in the brain. By varying the α parameter, different shaped of the utility function are defined. Testing different utility functions, an optimal solution to Eq. 3.6, 3.7, and 3.8 is found, yielding $\mathbf{d}^*$. The α that

minimizes the sum of the square error difference between the true PSC distribution and the simulated $d_{r,f}$ in all 50 areas is selected. In order to generalize the solution, the α is found for the average $d_{r,f}$ across the subjects and also across the conditions.

3.2   Example of Resource Allocation Mechanism

In this example we observe the resource distribution between four users ($R = 4$) when different levels of supply, S, are provided. First $\alpha = 1$ is defined for all r. However, equation (3.5) is not well defined for $\alpha_r = 1$. By considering the derivative of the utility function in the limit as $\alpha_r \to 1$

$$
\begin{aligned}
\lim_{\alpha \to 1} U_r'(d_r) &= \lim_{\alpha \to 1} w_r d_r^{-\alpha_r} \\
&= \frac{w_r}{d_r}
\end{aligned}
\tag{3.13}
$$

Calculating the integral of (3.13) leads to the utility function

$$
U_r(d_r) = w_r \ln(d_r)
\tag{3.14}
$$

The weights of the users are set to $w_r = [0.5, 1.0, 2.0, 3.0]$. Based on the utility functions, we want to maximize the social welfare by changing the resources allocated to each user, d_r, with a supply constraint:

$$
Maximize \quad \sum_R w_r \ln(d_r), \quad 1, .., , R = 4
\tag{3.15}
$$

$$
s.t. \quad \sum_R d_r \leq S
\tag{3.16}
$$

Without loss of generality we can set $\sum_R d_r = S$. The maximum of equation (3.15) with the constraint in equation (3.16) can be found through the use of Lagrangian multipliers

$$L(d_1, d_2, d_3, d_4, \lambda) = \sum_{r=1}^{4} w_r \ln(d_r) - \lambda \left(\sum_{r=1}^{4} d_r - S \right) \tag{3.17}$$

To find the maximum of L, we take the derivative with respect to d_r and set the result equation to zero

$$\frac{\partial L}{\partial d_r} = \frac{w_r}{d_r} - \lambda = 0 \tag{3.18}$$

therefore

$$d_r = \frac{w_r}{\lambda} \quad \forall r \tag{3.19}$$

Next, taking the the derivative of L in respect to λ and setting equal to zero

$$\frac{\partial L}{\partial \lambda} = \sum_{r=1}^{4} d_r - S = 0 \tag{3.20}$$

which yields:

$$\sum_{r=1}^{4} d_r = S \tag{3.21}$$

With the use of the four equations, one for each user, in (3.19) and equation (3.21) we can solve for the variables $(d_1, d_2, d_3, d_4, \lambda)$ based on the w_r's and S.

Different values of S (15, 50, 100, 250) were tested to evaluate the behavior of the resource allocation mechanism. Table 3.1 and Figure 3.2 show the change in distribution from different supply values. Table 3.1 shows the amount of resources that each of the four users received based on the supply available. As can be noted from these results, as the supply increases there is an increase for all users in the amount of resources that they receive. However, the users with higher utility weights receive an increase in greater proportion then the users with smaller weights. Additionally, as supply increases, there is a decrease in the value of λ. In some applications, λ is viewed as the price per unit of the supply [33]. In this perspective, as supply increases, the price per unit is a function of the inverse of the supply.

User	w	$S = 15$	$S = 50$	$S = 100$	$S = 250$
User 1	0.5	1.1538	3.8462	7.6923	19.2308
User 2	1.0	2.3077	7.6923	15.3846	38.4615
User 3	2.0	4.6154	15.3846	30.7692	76.9231
User 4	3.0	6.9231	23.0769	46.1538	115.3846
λ	-	0.4333	0.1300	0.0650	0.0260

Table 3.1: Example of resource allocation at different supply levels.

Figure 3.2 shows in each panel the resource allocation for 4 different supply values. The x-axis is the amount of resource that each user receives while the y-axis is the utility function of each user. The blue lines show the utility function of each user as a function of d_r. The red dots show the amount of resources that each user receives solving for equations (3.19) and (3.21) as a function of the supply.
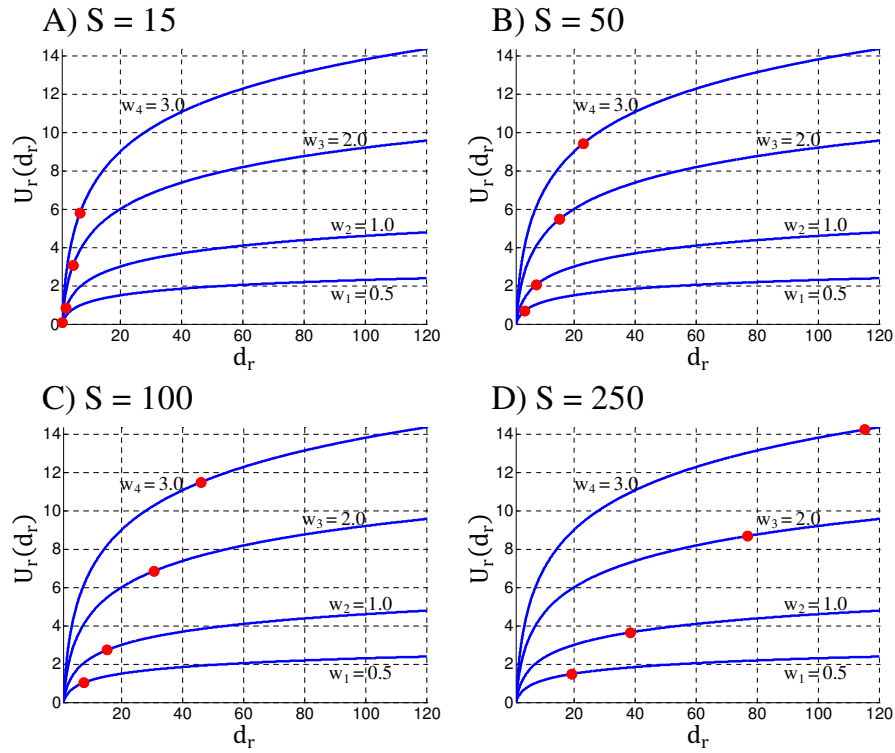
Figure 3.2: Example of resource allocation at different supply levels.

3.3   Creating Simulated Data

Simulations were performed to test the specificity and sensitivity of the proposed resource allocation model. Data was created to simulate brain activation in four different areas of the brain, including the auditory, visual, motor cortex and the posterior cingulate (PCC[1]). Simulated data in the three conditions of the Rate study (attend both, attend auditory or attend visual) were created with the use of real brain activation. Activation in the areas are based on the average measured whole brain activation (PSC) of each of the 15 subjects. With the whole brain activation of each subject at each condition, a specific percentage increase was attributed to the areas to simulate activation in each of the four areas. As an

---

[1]The PCC is known as one of the central hubs of the default mode network. These areas of the brain are known to deactivate when goal-oriented activity is being performed [37].

example, if the PSC of the whole brain is equal to 1, then in an area that has a 10% increase of activation, the PSC of that area will be 1.1 for that specific condition. Decrease of activation was also calculated using the same procedure. Table 3.2 specifies the percentage of increase or decrease of activation for each of the four areas at each condition. Paired t-tests were then performed to asses the ability to distinguish conditions using the resource allocation weighting factors, the direct PSC at each frequency, and also the slope. As an example, we would expect that the methods would be able to distinguish activation levels in the auditory cortex when the subjects are either attending to the auditory stimulus versus the visual stimulus. However, we would expect to not find any statistical difference in that same area when the subject is either attending to both stimuli or just the auditory stimulus.

Task	Auditory Cortex	Visual Cortex	Motor Cortex	PCC
Attend Both	3%	3%	2%	-5%
Attend Auditory	3%	0%	2%	-3%
Attend Visual	0%	3%	2%	-3%

Table 3.2: Simulation activation values.

3.4 Testing the Model

Several statistical tests were performed to asses the specificity and sensitivity of the resource allocation weighting factors as a method to asses neuronal activation. Statistical tests include one way ANOVAs and also paired t-tests [22]. Tests were also conducted to asses how well the proposed model is a feature extractor to perform classification between groups (NC vs. SZ and NC vs. mTBI). Classification was carried out using support vector machines (SVM; [10])

Chapter 4

Results

To asses the reliability of the resource allocation model, attention can be focused on some key areas of the brain where activation is expected to occur based on the stimuli of the two experiments. Both task require auditory and visual attention, as well as motor motion. Areas of interest in the brain include the auditory cortex [areas of the middle and superior temporal gyrus, and transverse temporal gryus, including Brodmannareas (BA) 41 and 42], the visual cortex [lingual gyrus, occipital lobe (BA 17, 18 and 19) and also some of the parietal lobe], primary motor [precentral gyrus (BA 4)] and also the two central hubs of the default mode network [anterior and posterior cingulate cortex]. Areas of the DMN are included in this list because they are known to reduce in activation when a cognitive demanding tasks are being performed.

In this chapter only results are shown, while a discussion of the implications of the presented results are addressed in chapter 5.

4.1 Rate Study

This section presents the results of using the weighting factors and also the other traditional methods to analyze FMRI in the Rate study. First, results of statistical tests on the simulated data (section 3.3) are shown. First, ANOVAS and t-tests are performed between stimuli conditions using the all the methods. Next, the α parameter from the utility function (Eq. 3.5) is selected to minimize the estimation error of the resource allocation model in relation to the subject data. Afterwords, the test are performed on the parameters to assess if they are normally distributed. If they are, then parametric statistical tests can be performed on these data. Subsequently, the weighting factors are calculated and statistical tests are performed between conditions for the NC. The same is also performed for the traditional methods. Then, independent t-tests are performed between groups (NC vs. mTBI) for each condition. Finally, classification between groups using support vector machines is done to assess the power if feature extraction of the resource allocation model.

4.1.1 Simulations

For a few subjects in some conditions, the average WB PSC was negative. This is unexpected, since there is a drop of WB hemodynamic response when the task is being performed compared to baseline. However, based on Eq. 3.8, the resource allocation model cannot be calculated with negative PSC. Therefore a constant (=0.3) was added to all WB PSC values. Table 4.1 shows the average PSC of the WB across the subjects for each condition and frequency. This is illustrated to show the variability in WB PSC based on the conditions and also intensity (frequency) of the tasks. Additionally, for the general utility function (Eq. 3.5) α is defined as $\alpha = 0.5$. Results were not affected by varying the constant and α values.

For each of the four simulated areas (auditory cortex, visual cortex, motor cortex, and

Stimuli Frequency	Stimuli Condition		
	Attend Both	Attend Auditory	Attend Visual
0.75 Hz	0.1139	0.0944	0.1450
1.25 Hz	0.1505	0.1397	0.1463
1.50 Hz	0.1715	0.1482	0.1782

Table 4.1: Average WB PSC across frequencies and stimuli conditions for the normal controls in the Rate study.

Method		1-way Anova				Attend Both vs Attend Auditory				Attend Both vs Attend Visual				Attend Auditory vs Attend Visual			
		Aud	Vis	Motor	PCC	Aud	Vis	Motor	PCC	Aud	Vis	Motor	PCC	Aud	Vis	Motor	PCC
w		$p < 0.001$	$p < 0.001$	$p > .1$	$p < 0.05$	$p > .1$	B>A $p < .001$	$p > .1$	A>B $p < .05$	B>V $p < .001$	$p > .1$	$p > .1$	V>B $p < .001$	A>V $p < .001$	V>A $p < .001$	$p > .1$	$p > .1$
PSC	.75Hz	$p > .1$	$p > .1$	$p > .1$	$p > .1$	$p > .1$	$p > .1$	$p > .1$	$p > .1$	$p > .1$	$p > .1$	$p > .1$	V>B $p < .1$	V>A $p < .05$	V>A $p < .05$	V>A $p < .05$	V>A $p < .05$
	1.25Hz	$p > .1$	$p > .1$	$p > .1$	$p > .1$	$p > .1$	$p > .1$	$p > .1$	$p > .1$	$p > .1$	$p > .1$	$p > .1$	$p > .1$	$p > .1$	$p > .1$	$p > .1$	$p > .1$
	1.5Hz	$p > .1$	$p > .1$	$p > .1$	$p > .1$	$p > .1$	$p > .1$	$p > .1$	$p > .1$	$p > .1$	$p > .1$	$p > .1$	$p > .1$	$p > .1$	$p > .1$	$p > .1$	$p > .1$
Slope		$p > .1$	$p > .1$	$p > .1$	$p > .1$	$p > .1$	$p > .1$	$p > .1$	$p > .1$	$p > .1$	$p > .1$	$p > .1$	$p > .1$	$p > .1$	$p > .1$	$p > .1$	$p > .1$

Table 4.2: Simulation results.

PCC), 1-way ANOVAS were performed across the three tasks. Paired t-tests between the conditions were also performed in each simulated area. Statistical p-values are shown in Table 4.2. As displayed in the Table 4.2, test were performed on the weighting factors (w), PSC at each frequency, and also on the slope. The directionality of the t-tests that show significant ($p < 0.05$) or a trend ($p < 0.1$) between conditions are indicated.

To further address the power of using the utility function weighting factor's as a measurement of brain's relative activation, different levels of gaussian noise were applied to the simulated signal. As previously, ANOVA tests where conducted but now at different gaussian noise levels. However, the experiments are repeated 500 times at each noise level. The noise levels tested ranged from an a signal to noise ratio (SNR) of 10 down to 0.33. As expected, no significance was found in the motor area in all levels of SNR. In the PCC area, significance ($p < 0.05$) was still found between the conditions in an SNR of 5. As for the auditory and visual areas, significance in the ANOVA was still present in a SNR as

low as 0.5.

4.1.2   Alpha of the Utility Function

Initially, the α parameter must be estimated for the associated utility functions (Eq. 3.5). To find a fixed α, first the average PSC across the 30 subjects (NC and SZ) for each of the 50 cortical areas were calculated for each condition. A constant ($= 2$) is added to all PSC to guarantee that all d_r values were not negative, therefore satisfying Eq. 3.8. Similar to the simulations, results did not change based on the constant applied to the PSC's. A range of α values ($0.001 \leq \alpha \leq 20$) were tested to estimate the final distribution of resources for each region d_r. First, for each α, the λ_f's were calculated. Then a solution for Eqs. 3.6, 3.7, and 3.8 was calculated for each α. Results where then compared to the true PSC of each of the 50 cortical areas. The average error across all three conditions were then averaged to select the α that best estimated the true distribution. The optimal value α value was found to be 2.287. Figure 4.1 shows the estimation error when varying the α for each condition and also the average error across all conditions.

4.2   Normality Tests of the Weighting Factors

One-Sample Kolmogorov-Smirnov tests were calculated to assess the distribution of the weighting factors in each of the 50 cortical areas. To compare, these tests were also performed on the PSC's (at each frequency) and the slope. The number of tests that rejected the null hypothesis ($p < 0.05$; data is not normally distributed) for the weighting factor are 3 (attend both), 2 (attend auditory), and 3 (attend visual) out of 50 areas. Considering the number of Kolmogorov-Smirnov tests, this is the expected number of tests (~ 2.5) that would indicate a non-gaussian distribution (Type-I error). As for the PSC's and the slope, a similar number of areas also did not pass the gaussianity test, ranging from 0 to
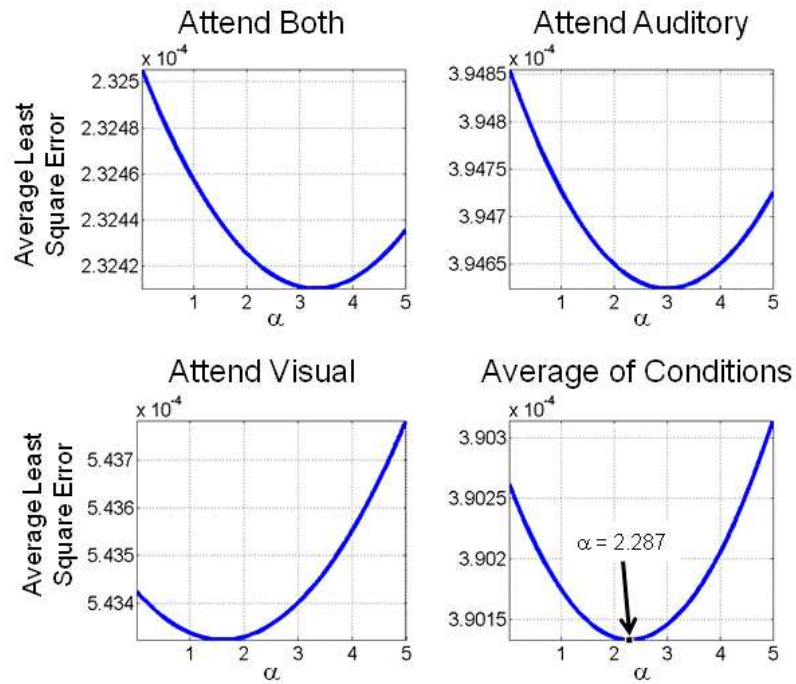
Figure 4.1: Minimizing estimation error by varying α of the utility function (Eq. 3.5.)

5 at each condition. Since the weighting factor from the utility functions are statistically considered to be gaussian distributions, parametric tests such as ANOVAS and t-tests can be performed on these data.

4.2.1 Weighting Factors of Normal Controls

After selecting the optimal α, the average weighting factor (w) from the utility function (Eq. 3.5) were calculated in each of the 50 areas for the three conditions (attend both, only auditory, and only visual). The values of the weights are shown in Table 4.3. These values were calculated from the average PSC of each area across the fifteen NC subjects.

Neuronal Area		Weighting Factor (w) of Cortical Area		
		Attend Both	Attend Auditory	Attend Visual
Cortical	Posterior Cingulate	0.9287	0.9089	0.9058
	Anterior Cingulate	0.7663	0.7619	0.7562
	Subcallosal Gyrus	0.8152	0.7902	0.7872
	Transverse Temporal Gyrus	1.142	1.1352	1.1004
	Uncus	0.8337	0.8222	0.8231
	Rectal Gyrus	1.0221	1.0084	1.0189
	Fusiform Gyrus	1.0556	1.0531	1.0614
	Inferior Occipital Gyrus	1.0987	1.061	1.0414
	Inferior Temporal Gyrus	0.9211	0.9207	0.9114
	Insula	1.0176	1.0247	1.0088
	Parahippocampal Gyrus	0.9109	0.9095	0.9072
	Lingual Gyrus	1.3747	1.3533	1.371
	Middle Occipital Gyrus	1.0702	1.0355	1.0854
	Orbital Gyrus	1.0652	1.0737	1.1197
	Middle Temporal Gyrus	0.8756	0.8817	0.8679
	Superior Temporal Gyrus	1.0068	1.014	0.9859
	Superior Occipital Gyrus	0.7821	0.7688	0.7833
	Inferior Frontal Gyrus	0.896	0.901	0.8995
	Cuneus	1.2434	1.2201	1.2421
	Angular Gyrus	0.8003	0.8114	0.7849
	Supramarginal Gyrus	0.9549	0.9759	0.958
	Cingulate Gyrus	0.9117	0.921	0.9129
	Inferior Parietal Lobule	1.0872	1.0914	1.0816
	Precuneus	0.9368	0.9398	0.9578
	Superior Parietal Lobule	0.9835	0.9731	1.0162
	Middle Frontal Gyrus	0.8912	0.9095	0.896
	Paracentral Lobule	0.8838	0.8747	0.8771
	Postcentral Gyrus	1.1704	1.1497	1.136
	Precentral Gyrus	1.1039	1.1032	1.1143
	Superior Frontal Gyrus	0.8407	0.8478	0.8322
	Medial Frontal Gyrus	0.863	0.8553	0.8495
Cerebellum	Uvula of Vermis	1.0633	1.0592	1.098
	Pyramis of Vermis	1.2318	1.2403	1.3295
	Tuber of Vermis	1.3244	1.3236	1.4184
	Declive of Vermis	1.7402	1.7304	1.8897
	Culmen of Vermis	1.6307	1.6065	1.6659
	Cerebellar Tonsil	1.0546	1.0582	1.0723
	Inferior Semi-Lunar Lobule	0.9711	0.9742	0.974
	Fastigium	1.1259	1.1265	1.1335
	Nodule	1.0535	1.0537	1.0668
	Uvula	1.2283	1.2387	1.2711
	Pyramis	1.1856	1.2015	1.2181
	Tuber	1.4011	1.445	1.4523
	Declive	1.4949	1.495	1.5482
	Culmen	1.2082	1.2029	1.2188
	Cerebellar Lingual	1.1039	1.1142	1.1093
Sub-cortical	Lentiform Nucleus	0.9838	0.9824	0.9809
	Claustrum	0.9922	0.997	0.9869
	Thalamus	0.9815	0.9863	0.9987
	Caudate	0.9083	0.9218	0.9187

Table 4.3: Utility function weighting factor (w) for each of the 50 cortical areas in each three conditions for normal controls in the Rate study.

4.2.2 Statistical Tests Between Conditions on Normal Controls

For each NC subject, the weighting factors in each neuronal area were calculated. With the weighting factors, fifty one-way ANOVAs (one for each area) across the three conditions were performed. Statistical results indicated that there were no significant differences ($p > 0.1$) between any of the conditions. One-way ANOVAs were also performed directly on the PSC at each frequency and also in the slope across the frequencies. The only statistically significant ($p < 0.05$) result that was found was in the PSC at 0.75 Hz in the middle occipital gyrus.

Even though there was not significance in the ANOVA in any of the areas using the weighting factors, several paired two-sample t-tests were computed. Tests were done to compare the three conditions (attend both vs. attend auditory; attend both vs. attend visual; attend auditory vs. attend visual). T-tests across the conditions with the PSC at each frequency and also the slope were also calculated. Results of all the t-tests are shown in Table 4.4, were the direction of tests that where significant ($p < 0.05$) are also indicated. Conditions include attend auditory and ignore visual (A), attend visual and ignore auditory (V), and attend both (B) stimuli. Statistical tests in bold are further examined in the discussion session. Neuronal areas that did not have any statistical significance are not shown.

4.2.3 T-tests Between Normal Controls and Patients with Schizophrenia

Independent t-tests were performed in all 50 areas to compare the weighting factors of NC and SZ. Results of using the weighting factor and the other methods are shown in Table 4.5. Significant t-tests ($p < 0.05$) are indicated in the table with the corresponding direction of the test. The bottom row indicates the total number of areas that showed

Neuronal Areas	Attend Both vs. Attend Auditory					Attend Both vs. Attend Visual					Attend Auditory vs. Attend Visual				
	w	PSC .75Hz	1.25Hz	1.50Hz	Slope	w	PSC .75Hz	1.25Hz	1.50Hz	Slope	w	PSC .75Hz	1.25Hz	1.50Hz	Slope
Posterior Cingulate	**B>A**			B > A		**B > V**									
Transverse Temporal Gyrus				**B > A**		**B > V**		**B > V**	**B > V**		**A > V**				
Uncus												V > A			
Fusiform Gyrus												V > A			
Inferior Occipital Gyrus		B > A				B > V				B > V					
Inferior Temporal Gyrus											A > V				
Lingual Gyrus				B > A								V > A		V > A	
Middle Occipital Gyrus	**B>A**	B > A		B > A							V > A	V > A	V > A	V > A	
Middle Temporal Gyrus						**B > V**					**A > V**				
Superior Temporal Gyrus						**B > V**					**A > V**				
Cuneus		B > A		B > A								V > A		V > A	
Angular Gyrus											A > V				
Supramarginal Gyrus	A>B						V > B				A > V				
Cingulate Gyrus							V > B								
Inferior Parietal Lobule				B > A											
Precuneus												V > A			
Superior Parietal Lobule				B > A			V > B				V > A	V > A		V > A	
Middle Frontal Gyrus	A>B										A > V				
Paracentral Lobule				B > A						B > V		V > A			
Postcentral Gyrus		B > A		B > A		**B > V**									
Precentral Gyrus							V > B					V > A			
Superior Frontal Gyrus											A > V				
Uvula of Vermis						V > B	V > B				V > A	V > A			
Pyramis of Vermis						V > B		V > B			V > A	V > A			
Tuber of Vermis						V > B	V > B	V > B			V > A	V > A			
Declive of Vermis						V > B	V > B	V > B	V > B		V > A	V > A		V > A	
Culmen of Vermis											V > A	V > A		V > A	
Cerebellar Tonsil						V > B	V > B					V > A			
Fastigium												V > A		V > A	
Nodule							V > B					V > A		V > A	
Uvula						V > B						V > A			
Tuber												V > A			
Declive							V > B				V > A	V > A			
Culmen												V > A		V > A	
Cerebellar Lingual									V > B					V > A	
Thalamus						V > B	V > B								
Caudate						V > B									
Total	4	4	0	9	0	14	11	4	3	2	16	21	1	10	0

Table 4.4: Paired t-tests between conditions for normal controls in the Rate study.

significant differences. Areas that did not exhibit any significant results for any of the four methods are removed from the table.

4.2.4 Classification Between Normal Controls and Patients with Schizophrenia

This section shows the results of performing classification between NC and SZ by using the weighting factors and the other method as features to distinguish between groups. Classification was performed independently at each stimuli condition (attend both, attend

Neuronal Areas	Attend Both					Attend Auditory					Attend Visual				
	w	PSC			Slope	w	PSC			Slope	w	PSC			Slope
		.75Hz	1.25Hz	1.5Hz			.75Hz	1.25Hz	1.5Hz			.75Hz	1.25Hz	1.5Hz	
Posterior Cingulate	NC>SZ	NC>SZ	NC>SZ	NC>SZ					NC>SZ		NC>SZ	NC>SZ	NC>SZ	NC>SZ	
Transverse Temporal Gyrus						SZ>NC									
Rectal Gyrus									NC>SZ						
Insula	SZ>NC					SZ>NC									
Superior Temporal Gyrus						SZ>NC									
Cuneus	NC>SZ	NC>SZ	NC>SZ	NC>SZ		NC>SZ	NC>SZ	NC>SZ	NC>SZ			NC>SZ	NC>SZ		
Supramarginal Gyrus					NC>SZ										
Inferior Parietal Lobule	SZ>NC					SZ>NC									
Precuneus	NC>SZ		NC>SZ	NC>SZ		NC>SZ			NC>SZ		NC>SZ	NC>SZ	NC>SZ		
Paracentral Lobule	SZ>NC					SZ>NC									
Postcentral Gyrus										NC>SZ					
Precentral Gyrus	SZ>NC					SZ>NC				NC>SZ	SZ>NC				
Culmen of Vermis												NC>SZ			
Tuber	NC>SZ	NC>SZ	NC>SZ	NC>SZ		NC>SZ	NC>SZ	NC>SZ	NC>SZ		NC>SZ	NC>SZ	NC>SZ		
Total	8	3	4	4	1	9	2	2	5	2	4	5	4	1	0

Table 4.5: Results from independent t-tests comparing NC versus SZ in the Rate study

auditory, and attend visual). A linear support vector machine (SVM) was used as a classifier [10]. A leave one out approach was used to evaluate the classification, where the classifier is built using data from all the subjects but one. The excluded subject is then tested with the classifier, labeling the subject a NC or a SZ. This process was repeated until all the 30 subjects were tested.

Initially, the features used in classification were the weighting factors of all the 50 areas. However, accuracy in classification between both groups was roughly around 50% (chance) for all methods and conditions. This is likely to be occurring from overfitting the network to the training dataset by using to many features. To increase the robustness, an adequate feature selection process is important in order to build a good classifier. Therefore to improve classification results, the feature set was reduced. Only areas that showed significant difference between groups (Table 4.5) were used as features in the classifier. As and example with the weighting factors, for the attend visual condition, only the posterior cingulate, precuneus, precentral gyrus and the tuber were used as features. For the other conditions and other methods, different areas were used as features. This is done such that each method is independently performing feature selection and classification. Classification accuracy is shown in Table 4.6.

Method		Attend Both	Attend Auditory	Attend Visual
w		73.33%	76.67%	60.00%
PSC	0.75Hz	63.33%	66.67%	60.00%
	1.25Hz	70.00%	53.33%	66.67%
	1.50Hz	56.67%	60.00%	60.00%
Slope		36.67%	50.00%	66.67%

Table 4.6: Classification accuracy between normal controls and patients with schizophrenia using linear support vector machine in the Rate study.

4.3   Multimodal Attention Task Study

For the MMAT study, several types of tests were performed to asses the advantage or disadvantage of using a resource allocation model to analyze FMRI data compared to traditional methods. Tests include; between conditions at the first FMRI session for NC, between groups at each condition and also at each visit, and also for NC and mTBI between their respective visits. Finally, classification using SVM was also performed on these analysis.

4.3.1   Alpha of the Utility Function

As previously done for the Rate study and seen in section 4.1.2, the alpha parameter of the utility function (Eq. 3.5) must be defined. First, a constant (=8) is added to the PSC to all conditions (None, Auditory, and Visual), frequency frequency (0.33 and 0.66 Hz) and subjects (NC and mTBI). This constant is larger then for the Rate study since it is based on the smallest PSC value of the study data across all subjects and conditions. The ideal α was found to be equal to 1.288.

4.3.2 Statistical Tests Between Conditions on Normal Controls

With the weighting factors calculated for the NC, parametric tests (ANOVA and paired t-tests) were performed across conditions. Fifty ANOVAS (between conditions) where first performed on the all neuronal areas. Follow up paired t-tests where then performed on the areas that showed significance ($p < 0.05$) on the ANOVA. Results of the followup tests that where also significant ($p < 0.05$) are presented in Table 4.7. Directionality of the tests are shown, for all the conditions including attending none (N), attending auditory (A) and also attending visual (V). As before, only the areas that passed the tests are shown. Additionally, test in bold text are further addressed in the discussion chapter (chapter 5).

4.3.3 T-tests Between Normal Controls and Mild Traumatic Brain Injury Patients

Initially a 2-way ANOVA (Condition x Subject) was performed. Of the 50 areas there were no interaction effect ($p > .1$) in any of the neuronal areas using the weighting factor or using directly the PSC at both frequencies. However, for the slope, the middle frontal gyrus showed a interaction effect ($p < 0.05$) of condition.

Even though there are no interaction effects for the weighting factors and the PSC, followup t-tests where still performed in all areas to asses the proposed method. Table 4.8 ilustrated the results the group differences for the first visit of NC and mTBI. There are a total of 24 subjects used in this analysis (12 per group). Table 4.9 refers to the same tests but now in reference to the subjects second visit. Only a subset of subject participated in the second visit (N=10).

Neuronal Area	None vs Auditory				None vs Visual				Auditory vs Visual			
	w	.33Hz	.66Hz	slope	w	.33Hz	.66Hz	slope	w	.33Hz	.66Hz	slope
Posterior Cingulate				N>A								
Anterior Cingulate	**N>A**				**N>V**							
Fusiform Gyrus				N>A								V>A
Parahippocampal Gyrus	N>A			N>A	N>V							V>A
Middle Occipital Gyrus	N>A				**N>V**				V>A			
Middle Temporal Gyrus	**N>A**				N>V							
Superior Occipital Gyrus												V>A
Inferior Frontal Gyrus				N>A								V>A
Angular Gyrus	N>A			N>A	N>V				V>A			V>A
Supramarginal Gyrus		A>N		N>A		V>N				A>V		V>A
Cingulate Gyrus												V>A
Inferior Parietal Lobule		A>N	A>N			V>N	V>N	V>N		A>V	V>A	V>A
Precuneus				N>A								V>A
Middle Frontal Gyrus		A>N								A>V		V>A
Paracentral Lobule				N>A								V>A
Postcentral Gyrus								V>N				V>A
Precentral Gyrus			A>N				V>N	V>N			V>A	V>A
Superior Frontal Gyrus				N>A								V>A
Medial Frontal Gyrus				N>A								V>A
Uvula of Vermis	A>N	A>N	A>N		V>N	V>N	V>N				V>A	
Pyramis of Vermis	A>N	A>N			V>N	V>N						V>A
Tuber of Vermis	A>N	A>N	A>N		V>N	V>N	V>N				V>A	V>A
Declive of Vermis	A>N	A>N	A>N		V>N	V>N	V>N				V>A	V>A
Cerebellar Tonsil		A>N	A>N			V>N	V>N			A>V		
Fastigium		A>N	A>N			V>N	V>N					
Nodule		A>N	A>N			V>N	V>N				V>A	V>A
Uvula		A>N				V>N						V>A
Declive		A>N	A>N			V>N	V>N				V>A	V>A
Culmen	A>N	A>N	A>N		V>N	V>N	V>N					
Cerebellar Lingual		A>N	A>N			V>N	V>N					
Lentiform Nucleus		A>N	A>N			V>N	V>N					V>A
Thalamus	A>N	A>N	A>N		V>N	V>N	V>N	V>N			V>A	V>A
Total	11	16	13	10	11	15	13	4	2	4	8	23

Table 4.7: Statistical test between conditions for the normal controls in the MMAT study.

4.3.4 Statistical Tests Between Visits

This section describes results of comparing the weighting factors of the subject between the first and second visit. Therefore, at each conditions, a paired t-test were done for all subjects between their first (V1) and second (V2) visit. Results are separated by groups. Ten subjects in each group where used in these tests. Significant results ($p < 0.05$) are shown for NC (Table 4.10) and mTBI (Table 4.11).

43

Neuronal Area	None				Auditory				Visual			
	w	PSC .33Hz	PSC .66Hz	Slope	w	PSC .33Hz	PSC .66Hz	Slope	w	PSC .33Hz	PSC .66Hz	Slope
Transverse Temporal Gyrus												mTBI>NC
Parahippocampal Gyrus			mTBI>NC									
Middle Occipital Gyrus									mTBI>NC			
Inferior Frontal Gyrus								mTBI>NC				
Inferior Parietal Lobule			mTBI>NC									
Precuneus			mTBI>NC						NC>mTBI			
Superior Parietal Lobule			mTBI>NC									
Middle Frontal Gyrus					mTBI>NC							
Paracentral Lobule	NC>mTBI											
Tuber of Vermis					NC>mTBI	NC>mTBI	NC>mTBI					
Declive of Vermis					NC>mTBI	NC>mTBI						
Uvula					NC>mTBI	NC>mTBI			NC>mTBI			
Pyramis					NC>mTBI	NC>mTBI	NC>mTBI					
Tuber					NC>mTBI							
Declive					NC>mTBI	NC>mTBI			NC>mTBI			
Lentiform Nucleus								mTBI>NC				
Total	1	0	0	4	7	5	2	2	4	0	0	1

Table 4.8: Independent t-tests between normal controls and mild traumatic brain injury patients for the first visit in the MMAT study.

Neuronal Area	None				Auditory				Visual			
	w	PSC .33Hz	PSC .66Hz	Slope	w	PSC .33Hz	PSC .66Hz	Slope	w	PSC .33Hz	PSC .66Hz	Slope
Uncus	mTBI>NC	mTBI>NC	mTBI>NC		mTBI>NC	mTBI>NC	mTBI>NC		mTBI>NC	mTBI>NC	mTBI>NC	
Lingual Gyrus					NC>mTBI							
Middle Frontal Gyrus	mTBI>NC											
Culmen					NC>mTBI							
Total	1	1	1	0	3	1	1	0	1	1	1	0

Table 4.9: Independent t-tests between normal controls and mild traumatic brain injury patients for the second visit in the MMAT study.

4.3.5 Classification Between Normal Controls and Mild Traumatic Brain Injury Patients

In this section, results of classification between groups and also within groups comparing visits is shown. For the classification between subjects, SVM is used for the first visit and

Neuronal Area	None				Auditory				Visual			
	w	PSC .33Hz	PSC .66Hz	Slope	w	PSC .33Hz	PSC .66Hz	Slope	w	PSC .33Hz	PSC .66Hz	Slope
Rectal Gyrus		V1>V2										
Parahippocampal Gyrus						V1>V2				V1>V2		
Orbital Gyrus					V1>V2	V1>V2						
Middle Temporal Gyrus	V2>V1											
Superior Occipital Gyrus						V1>V2						
Pyramis of Vermis						V1>V2						
Pyramis						V1>V2						
Lentiform Nucleus									V2>V1			
Caudate									V2>V1			
Total	1	1	0	0	1	5	0	0	2	1	0	0

Table 4.10: Paired t-tests between visits for normal controls in the MMAT study.

Neuronal Area	None				Auditory				Visual			
	w	PSC .33Hz	PSC .66Hz	Slope	w	PSC .33Hz	PSC .66Hz	Slope	w	PSC .33Hz	PSC .66Hz	Slope
Posterior Cingulate			V1>V2									
Transverse Temporal Gyrus	V1>V2	V1>V2	V1>V2		V1>V2				V1>V2			
Insula		V1>V2										
Superior Temporal Gyrus		V1>V2										
Postcentral Gyrus			V1>V2									
Inferior Semi-Lunar Lobule					V2>V1							
Culmen					V1>V2							
Thalamus	V2>V1											
Total	2	3	3	0	3	0	0	0	1	0	0	0

Table 4.11: Paired t-tests between visits for mild traumatic brain injury patients in the MMAT study.

Method		Attend None	Attend Auditory	Attend Visual
w		54.17%	66.67%	66.67%
PSC	0.33Hz	-	58.33%	-
PSC	0.66Hz	-	41.67%	-
Slope		66.67%	66.67%	66.67%

Table 4.12: Classification accuracy between groups (NC versus mTBI) for the first visit on the MMAT study.

also at the second visit. Based on the hypothesis presented in Figure 1.2, it is expected that there are more significant differences between groups in the first FMRI session while much less for the second session. Results of these tests for the first and second visit are shown in Tables 4.12 and 4.13 respectively. Similarly as the Rate study classification procedure, only areas that passes statistical tests (Tables 4.8 through 4.11) where used as features. Therefore, for some methods, no classification was performed since there are no significant differences in any of the neuronal areas.

The final set of classification results are shown in Tables 4.14 and 4.15. The first table shows classification accuracy when comparing the features of NC at their first visit versus their second visit. For all methods, an accuracy around 50% (chance) is expected since NC should have no change in brain resource allocation. As for Table 4.15, classification is performed between the first and second visit of the mTBI subjects.

Method		Attend Non	Attend Auditory	Attend Visual
w		55.00%	60.00%	65.00%
PSC	0.33Hz	55.00%	65.00%	60.00%
	0.66Hz	55.00%	60.00%	60.00%
Slope		-	-	-

Table 4.13: Classification accuracy between groups (NC versus mTBI) for the second visit on the MMAT study.

Method		Attend Non	Attend Auditory	Attend Visual
w		55.00%	70.00%	75.00%
PSC	0.33Hz	60.00%	75.00%	75.00%
	0.66Hz	-	-	-
Slope		-	-	-

Table 4.14: Classification accuracy between visits for the normal controls on the MMAT study.

Method		Attend Non	Attend Auditory	Attend Visual
w		50.00%	60.00%	60.00%
PSC	0.33Hz	65.00%	-	-
	0.66Hz	70.00%	-	-
Slope		-	-	-

Table 4.15: Classification accuracy between visits for the mild traumatic brain injury patients on the MMAT study.

Chapter 5

Discussion

A novel method to analysis FMRI data is proposed. The method assumes that there is an underlying resource allocation mechanism that distributes resources (oxygen and glucose) throughout the brain. A resource allocation model was used to describe activation of brain regions, where in a financial setting or in communication networks, competitive reasoning is used to find an optimal distribution of resources between users. In FMRI, the proposed model could potentially be used to study more in depth brain functionality.

With the use of the theoretical competitive equilibrium approach, we have mathematically equated a model that describes the fundamentals of resource allocation of the brain. The equations are based on a measurement of "importance" or "value" of receiving resources, defined by a utility function. By using the proposed model, the level of activation of brain regions is transformed to a relative measurement of activation. As described in chapter 3, the utility function of a specific cortical area of the brain changes based on the environment the subject is encountering, such as internal thoughts or a focusing on intense external stimuli. However, a strong assumption was proposed, where the brain always attempts to maximize the social welfare (Eq. 3.1) based on the conditions it is encountering. Basically, we are assuming that the brain is an efficient machine that always attempts to

minimize the energy loss [1].

A discussion of the all the results and the findings of all the neuronal areas would seem impracticable. Therefore, we will focus on discussing some of the key findings based on the expected neuronal functioning dependent on the two studies. As stated in the introduction, this project is focused on the proposed resource allocation model, hence implications of group differences will not be addressed in depth in this dissertation. Additionally, most of the discussions will be based on the cortical areas, abstaining to discuss much about cerebellum and also sub-cortical areas.

5.1   Rate Study

5.1.1   Simulations

Simulation tests indicated that the proposed resource allocation method is ideal to asses relative activation throughout the brain (Table 4.2). Based on the results from the 1-way ANOVA, only the resource allocation model was capable of finding the expected significant difference between all the attended conditions in the auditory cortex, visual cortex and the PCC. As expected, no significant difference between conditions were observed in the motor area. Additionally, the t-test comparing attend auditory versus attend visual, using directly the PSC at 0.75 Hz, there is always significant larger activation to attending the visual condition. Since we created the simulated data, we would expect different results in the auditory and PCC areas. They should be equal or similar to the weighting factors results. This simulation validates the capability of the proposed method in discovering relative activation throughout the cortical brain areas.

5.1.2   Statistical Tests Between Conditions on Normal Controls

A discussion of section 4.2.2 is presented in this section. Based on findings from table 4.4, there are some key areas that deserve a more in depth discussion. Some cortical areas of the brain are expected to have significantly different levels of activation based on what condition the subjects are attending to. More specifically, we would expect that the proposed method would find significant differences in the auditory and visual cortex across the conditions. Even though there are no significant results from the ANOVA tests, we assessed the difference in models the differences using paired t-tests. The middle and superior temporal gyri are well known for their roll in auditory processing, however, there is no significant level of activation detected by either the PSC at each frequency or either the slope. On the other hand, the resource allocation model finds significant difference in the weighting factor when either the subject is required to attend the auditory stimulus or both stimuli versus attending only the visual stimulus. This is a clear indication of a higher sensitivity of the proposed method. Additionally, the transverse temporal gyrus (BA 41 and 42 - primary auditory cortex) also shows the same directionality of the statistical tests using the weighting factors. However, for the PSC at 1.25 and 1.50 Hz when comparing the attend both versus the attend visual, the expected directionality of the statistical test is also found. Despite these results, a surprising results is also seen in the PSC at 1.50 Hz, were the attend both shows greater activation then the attend auditory condition.

Areas of the brain responsible for visual processing include the occipital lobe, fusiform gyrus and cuneus. The middle occipital gyrus shown significantly larger weighting factors for attending visual and also attending both modalities versus only attending the auditory stimulus. However in the inferior occipital gyrus the model showed that there is a larger weighting factor when the subjects are attending both conditions rather then just attending the visual stimuli. Even though not significant and just showing trend ($p < 0.1$), looking at Table 4.3 there is a larger weighting factor for the attend visual and also attend both compared to attend auditory. The same holds for the cuneus. These results indicate that

the proposed method can be used to asses an "importance" measurement of neuronal areas based on the condition.

Additionally, the weighting factor found statistical differences in the posterior cingulate, where the attend to both condition is always higher then attending to only a single stimulus. The posterior cingulate cortex (PCC) is known as one of the central hubs of the default mode networks, where there is a decrease in neuronal activation when a goal-oriented activity is being performed. By observing Table 4.3, it can be seen that weighting factors from in the PCC are all below 1. This is indicative that the the "importance" of this area is decreased as the stimuli are being presented. However, there is a larger decrease when attending to a specific condition, rather then attending both. Attending to one condition while ignoring the other condition requires larger concentration from the subjects, therefore "stealing" more resources from areas that are not in much need.

These findings are based on several t-test that were not corrected for multiple comparisons. However, this dissertation is not assessing directly cortical brain functionality based on used stimuli, this can be seen in [30], but it is a project to asses the proposed method, where results clearly indicate that the proposed method is more sensitive to the different conditions compared to the traditional methods for the Rate study.

Finally, by observing Table 4.1, it can be seen that the attend visual always has a greater average WB PSC in all the stimuli frequency when comparing to the attend auditory. This has caused in the comparison between attending visual versus attending auditory, all the significant findings are attend visual greater then attend auditory in all the frequencies (Table 4.4). Relative neuronal activation is not observed when using directly the PSC, unlike the resource allocation method.

5.1.3   Group Differences and Classification

This section discusses the results from Tables 4.5 and 4.6 Clearly, when comparing the attend both condition versus the other two conditions, the resource allocation method finds the most difference between groups in neuronal areas. Another major observation from Table 4.5, is that there is no specificity when comparing groups while using the traditional methods. For all statistical significant results, NC always show greater activation than SZ. By using the resource allocation's weighting factor as a measurement of neuronal activation results show that nearly half of the significant differences between groups show greater activation for SZ compared to NC.

The accuracy of the classification using SVM's are low when using all the neuronal areas as features to find which group the subject belongs to. This is likely due to overfitting the training dataset. Therefore only using the areas that passed the statistical threshold ($p < 0.05$) in Table 4.5 are used as features. Also, using a conjunction of the methods for the classifier was not performed since we are evaluating the capabilities of each individual method. Therefore each of the methods must preform classification by itself, where a combination across methods is highly likely to increase classification accuracy. Results from Table 4.6 show that the resource allocation method clearly outperforms the other methods in group classification when using the attend both (73.33%) and attend auditory (76.67%) conditions. For the attend visual condition, all methods exhibit similar classification results.

5.2 MMAT study

5.2.1 Statistical Tests Between Conditions on Normal Controls

This section will address results of each of the methods when comparing across conditions (attend none, auditory, and visual) in normal controls for the MMAT study (see Table 4.7). The first result to note is that the resource allocation method is the only methods that accurately locates the anterior cingulate as having significant difference in activation when the subjects are instructed to attend to a specific modality versus attending none. While attending to the task, a reduced activation in this central hub of the DMN is expected compared to when the subject is instructed to not attend to any modality. The resource allocation method was the only method to accurately find significant difference across these conditions. There was also significance (p<0.001) in the posterior cingulate for the weighting factor (N > A and V), however there was only a trend (p<0.1) for the effect of condition from the ANOVA, therefore the result is not shown in the table. However, there are some unexpected results from using the weighting factors as a neuronal activation measurement, possibly a false positive (type I error). The none condition shows a greater weighting factor then the attend visual condition in the middle occipital gyrus (areas responsible for visual processing). Another unexpected result is seen in the middle temporal gyrus, where now the attend none has a greater weighting factor then the attend auditory.

Another significant finding from Table 4.7 is that most of the significant difference between conditions for all methods is seen in subcortical and cerebellar regions. When using directly the PSC in the two frequencies (0.33 and 0.66 Hz) as a measurement of neuronal activation a general pattern is observed. For all t-tests, the attend none condition is always showing lower hemodynamic response compared to both attending conditions (auditory and visual). The slope method finds the most cortical areas with significant difference, however there are no specificity in the findings. A general pattern [attend visual > attend auditory > attend none] is seen across the significant findings in the neuronal

areas.

5.2.2   Group Differences and Classification

First we will address results from Tables 4.8 and 4.12, where neuronal activation between NC and mTBI are compared for the subjects first FMRI session. Based on these results, the performance of the resource allocation method is not as robust to compare groups as was observed in the Rate study. In only a few cortical areas there was any significant differences between groups. As a result, the accuracy of the classification in lower then before ($< 67\%$). However, for the other methods (PSC's and slope) results are of similar or of inferior quality then the resource allocation. The classification between groups using the PSC's and slope are of similar accuracy compared to the weighting factors. Nonetheless, by only using directly the PSC, there are no significant findings between group in cortical brain areas where all results are located in the cerebellum. The slope however does find some significant differences between groups in cortical areas as well as cerebellar and subcortical areas of the brain.

As expected from the theoretical equilibrium pipeline (Figure 1.2), there is a general decrease in differences of neuronal activation between groups (see Tables 4.9 and 4.13). Even though there is no significant decrease in classification accuracy, there is a large decrease in neuronal areas that are significantly different between groups for all conditions. These results postulate two theories, either the proposed equilibrium is a alternative to explain this effect or the decrease in number of subject (N=10) has decreased the significance between groups.

The final set of results from this dissertation is comparing neuronal activation of subjects between their first and second FMRI session. Results for NC can be seen in Tables 4.10 and 4.14, while results for mTBI are shown in Tables 4.11 and 4.15. Based on the equilibrium hypothesis (Figure 1.2), no differences between visits will be found for NC,

while there will be significant differences for the mTBI. For the NC, the PSC at 0.66 Hz and the slope outperform the resource allocation method and also the PSC at 0.33 Hz, since they do not find any differences between visits, therefore no classification can be performed for these methods. Differences found between visits for the NC are possibly due to the fact that the subjects are now accustomed to the FMRI environment and less overall neuronal activation occurs. Additionally, as noted from Table 4.14, classification results between visits are very similar for the resource allocation method and the PSC at 0.33 Hz. As for the patient group, significant difference between visits is only found in the attend none condition when using the PSC as a measurement of neuronal activation. The resource allocation finds differences between visits in all of the three conditions. Therefore, by following the proposed feature extraction pipeline, in only the resource allocation method can we perform classification in all the conditions. However, the best classification result is seen of the PSC at 0.66 Hz for the attend none condition. Slope does not find any differences between visits for NC, however, no differences are also found between visits for the patients. These poor results might also be due to the low amount of subjects per group that are being used (N = 10).

5.3   Conclusions

Result from the Rate study have indicated that the proposed resource allocation method accurately finds differences between conditions in areas of the brain that where expected to behave differently dependent on the condition. The traditional methods such as using directly the PSC and also the slope of activation are outperformed by using the weighting factors as measurements of neuronal activation. Also, classification between groups is improved with the resource allocation method, showing the potential as a feature extraction tool with increased sensitivity. A possible argument of why the proposed model is more sensitive in some cortical areas relative to the other two methods (direct PSC and slope),

is that an absolute activation level to perform tests is not being used, while a relative value of activation in relation to WB activation is being exploited. To find the λ parameter, we define the WB as a user and set the weighting factor equal to one, and later solve for λ (Eq. 3.11). With the calculated λ, the weighting factors of the cortical areas can also be calculated. Areas that have the exact same level of activation (PSC) as the average of the whole brain will have an $w_{WB} = 1$. Also, any area with greater activation than the average of the brain will have a $w_r > 1$, and less activation will have $w_r < 1$. Additionally, the computing of λ's are done on a subject-by-subject basis. Therefore the weighting factors are relative to the individual subjects' WB activation. This decreases the data inter-subject variability such as correcting for subjects that have a very low or very high level of activation throughout the brain.

Another advantage of the proposed method is that it is a measurement throughout the frequencies without the assumption that the hemodynamic response is linear relative to the rate of the stimulus. The model is based on the relationship of a whole brain signal, and how the resources are distributed. The slope method is a summery of activation through-out the frequencies, however, it assumes a direct linear relationship of the hemodynamic response. Results from Table 4.4, indicate that the slope method is the least sensitive of the methods when comparing to the three Rate study conditions.

For the MMAT study, the proposed model demonstrated satisfactorily results, where some expected difference between conditions, visits and groups are captured using the weighting factors. However, the other methods did not outperform the resource allocation model.

5.4 Future Work

Further research with other FMRI experiments can be performed could extend the applicability of the new method. Additionally, the proposed method can be used with positron emission tomography (PET) data, which directly measures resources being supplied to areas brain, such as glucose. The methods can also be expanded to other imaging modalities such as Magnetoencephalography (MEG) and Electroencephalography (EEG)

Further testing with the proposed model can still be carried out with other experimental design paradigms. Both experiments used to asses the resource allocation methods are block design paradigms, while an event-related design still needs to be evaluated.

The proposed model only uses a level of relative activation in relation to the task as a parameter of resources. Also, only a summery of the average activation throughout the experiment is used (PSC). However, the resource allocation model could be further extended to a TR-by-TR framework. Where the equilibrium of brain is analyzed at each TR. With this extension, resource allocation of resting state data can be studied. Also, the use of independent component analysis (ICA; [7]) could also be used as a measurement of resource allocation to study the resting state networks. The empirical z-score of the components would substitute the PSC used in the current framework.

Finally, this model should be tested with other clinical populations, such as patients with developmental, neurological, or psychiatric disorders.

References

[1] S. Achard and E. Bullmore. Efficiency and cost of economical brain functional networks. *PLoS Computational Biology*, 3:174–183, 2007.

[2] L. Amaral and J. Ottino. Complex networks. *The European Physical Journal B - Condensed Matter and Complex Systems*, 38(2):147–162, March 2004.

[3] B. A. Ardekani, A. H. Bachman, and J. A. Helpern. A quantitative comparison of motion detection algorithms in fmri. *Magn Reson Imaging*, 19(7):959–963, Sep 2001.

[4] D. S. Bassett and E. Bullmore. Small-world brain networks. *Neuroscientist*, 12(6):512–523, Dec 2006.

[5] H. G. Belanger, R. D. Vanderploeg, G. Curtiss, and D. L. Warden. Recent neuroimaging techniques in mild traumatic brain injury. *J Neuropsychiatry Clin Neurosci*, 19(1):5–20, 2007.

[6] M. A. Burock, R. L. Buckner, M. G. Woldorff, B. R. Rosen, and A. M. Dale. Randomized event-related experimental designs allow for extremely rapid presentation rates using functional mri. *Neuroreport*, 9(16):3735–3739, Nov 1998.

[7] V. D. Calhoun, T. Adali, G. D. Pearlson, and J. J. Pekar. A method for making group inferences from functional mri data using independent component analysis. *Hum Brain Mapp*, 14(3):140–151, Nov 2001.

[8] B. J. Casey, N. Tottenham, C. Liston, and S. Durston. Imaging the developing brain: what have we learned about cognitive development? *Trends Cogn Sci*, 9(3):104–110, Mar 2005.

[9] B. J. Casey, R. J. Trainor, J. L. Orendi, A. B. Schubert, L. E. Nystrom, J. N. Giedd, F. X. Castellanos, J. V. Haxby, D. C. Noll, J. D. Cohen, S. D. Forman, R. E. Dahl, and J. L. Rapoport. A developmental functional mri study of prefrontal activation during

References

performance of a go-no-go task. *Journal of Cognitive Neuroscience*, 9(6):835–847, 1997.

[10] C. Cortes and V. Vapnik. Support-vector networks. *Machine Learning*, 20(3):273–297, 1995.

[11] R. W. Cox. Afni: software for analysis and visualization of functional magnetic resonance neuroimages. *Comput Biomed Res*, 29(3):162–173, Jun 1996.

[12] R. W. Cox and A. Jesmanowicz. Real-time 3d image registration for functional mri. *Magn Reson Med*, 42(6):1014–1018, Dec 1999.

[13] R. S. Desikan, F. Ségonne, B. Fischl, B. T. Quinn, B. C. Dickerson, D. Blacker, R. L. Buckner, A. M. Dale, R. P. Maguire, B. T. Hyman, M. S. Albert, and R. J. Killiany. An automated labeling system for subdividing the human cerebral cortex on mri scans into gyral based regions of interest. *Neuroimage*, 31(3):968–980, Jul 2006.

[14] P. E. Dux, M. N. Tombu, S. Harrison, B. P. Rogers, F. Tong, and R. Marois. Training improves multitasking performance by increasing the speed of information processing in human prefrontal cortex. *Neuron*, 63(1):127–138, Jul 2009.

[15] H. Everett III. Generalized lagrange multiplier method for solving problems of optimum allocation of resources. *Operations Research*, 11(3):399–417, 1963.

[16] W. Fias, B. Reynvoet, and M. Brysbaert. Are arabic numerals processed as pictures in a stroop interference task? *Psychol Res*, 65(4):242–249, Nov 2001.

[17] K. J. Friston, A. P. Holmes, J. B. Poline, P. J. Grasby, S. C. Williams, R. S. Frackowiak, and R. Turner. Analysis of fmri time-series revisited. *Neuroimage*, 2(1):45–53, Mar 1995.

[18] G. H. Glover. Deconvolution of impulse response in event-related bold fmri. *Neuroimage*, 9(4):416–429, Apr 1999.

[19] P. Hagmann, L. Cammoun, X. Gigandet, R. Meuli, C. J. Honey, V. J. Wedeen, and O. Sporns. Mapping the structural core of human cerebral cortex. *PLoS Biol*, 6(7):e159, Jul 2008.

[20] L. Hurwicz. The design of mechanisms for resource allocation. *The American Economic Review*, 63:1–30, 1973.

[21] M. Jenkinson and S. Smith. A global optimisation method for robust affine registration of brain images. *Med Image Anal*, 5(2):143–156, Jun 2001.

References

[22] P. Jezzard, P. M. Matthews, and S. M. Smith, editors. *Functional MRI: an introduction to methods*. Oxford University Press, 2001.

[23] J. H. Kaas. Plasticity of sensory and motor maps in adult mammals. *Annu Rev Neurosci*, 14:137–167, 1991.

[24] A. M. C. Kelly, L. Q. Uddin, B. B. Biswal, F. X. Castellanos, and M. P. Milham. Competition between functional brain networks mediates behavioral variability. *Neuroimage*, 39(1):527–537, Jan 2008.

[25] F. P. Kelly, A. K. Maulloo, and D. K. H. Tan. Rate control for communication networks: Shadow prices, proportional fairness and stability. *The Journal of the Operational Research Society*, 49(3):237–252, 1998.

[26] B. Kolb and I. Q. Whishaw. *Fundamentals of Human Neuropsychology*. Worth Publishers, 6th edition, 2008.

[27] S. B. Laughlin and T. J. Sejnowski. Communication in neuronal networks. *Science*, 301(5641):1870–1874, Sep 2003.

[28] D. A. Lewis and P. Levitt. Schizophrenia as a disorder of neurodevelopment. *Annu Rev Neurosci*, 25:409–432, 2002.

[29] R. Marois and J. Ivanoff. Capacity limits of information processing in the brain. *Trends Cogn Sci*, 9(6):296–305, Jun 2005.

[30] A. R. Mayer, A. R. Franco, J. Canive, and D. L. Harrington. The effects of stimulus modality and frequency of stimulus presentation on cross-modal distraction. *Cereb Cortex*, 19(5):993–1007, May 2009.

[31] A. R. Mayer, A. R. Franco, J. Ling, and J. M. Cañive. Assessment and quantification of head motion in neuropsychiatric functional imaging research as applied to schizophrenia. *J Int Neuropsychol Soc*, 13(5):839–845, Sep 2007.

[32] T. W. McAllister, L. A. Flashman, B. C. McDonald, and A. J. Saykin. Mechanisms of working memory dysfunction after mild and moderate tbi: evidence from functional mri and neurogenetics. *J Neurotrauma*, 23(10):1450–1467, Oct 2006.

[33] N. Nisan, T. Roughgarden, E. Tardos, and V. V. Vazirani, editors. *Algorithmic Game Theory*. Cambridge University Press, 2007.

[34] D. A. Norman and D. G. Babrow. On data-limited abd resource-limited processes. *Cognitive Psychology*, 7:44–64, 1975.

References

[35] R. C. Oldfield. The assessment and analysis of handedness: the edinburgh inventory. *Neuropsychologia*, 9(1):97–113, Mar 1971.

[36] T. Parrish. Functional mr imaging. *Magn Reson Imaging Clin N Am*, 7(4):765–82, vi, Nov 1999.

[37] M. E. Raichle and A. Z. Snyder. A default mode of brain function: a brief history of an evolving idea. *Neuroimage*, 37(4):1083–90; discussion 1097–9, Oct 2007.

[38] S. M. Rao, P. A. Bandettini, J. R. Binder, J. A. Bobholz, T. A. Hammeke, E. A. Stein, and J. S. Hyde. Relationship between finger movement rate and functional magnetic resonance signal change in human primary motor cortex. *J Cereb Blood Flow Metab*, 16(6):1250–1254, Nov 1996.

[39] O. Sporns and C. J. Honey. Small worlds inside big brains. *Proc Natl Acad Sci U S A*, 103(51):19219–19220, Dec 2006.

[40] R. Srikant. *The Mathematics of Internet Congestion Control*. Birkhäuser Boston, 2003.

[41] J. Talairach and P. Tournoux. *Co-planar Stereotaxic Atlas of the Human Brain*. Thieme Publishing Group, 1988.